Linking the Mediterranean MIS 5 tephra markers to the Campi Flegrei 109-92 ka explosive activity (southern Italy) and refining the chronology of the MIS 5c-d millennial-scale climate variability

Monaco, L.[1,*], Giaccio, B.[2-3], Palladino, D.M.[1], Albert, P.G.[4], Arienzo, I.[6], Conticelli, S.[2-7], Di Vito, M.[5], Fabbrizio, A.[8], D'Antonio, M.[9], Isaia, R.[5], Manning, C.J.[10], Nomade, S.[11], Pereira, A.[12], Petrosino, P.[9], Sottili, G.[1], Sulpizio, R.[13], Zanchetta, G.[2-7-14].

1 Dipartimento di Scienze della Terra, "Sapienza" Università di Roma, Rome, Italy
2 Istituto di Geologia Ambientale e Geoingegneria, CNR, Rome, Italy
3 Istituto Nazionale di Geofisica e Vulcanologia, INGV, Rome, Italy
4 Department of Geography, Swansea University, Swansea, UK
5 Istituto Nazionale di Geofisica e Vulcanologia, INGV-Osservatorio Vesuviano, Naples, Italy
6 Dipartimento di Scienze della Terra, Università degli Studi di Firenze, Florence, Italy
7 Istituto di Geologia Ambientale e Geoingegneria, IGAG-CNR, Rome, Italy
8 Institute of Petrology and Structural Geology, Faculty of Science, Charles University, Albertov 6, 12843 Prague, Czech Republic
9 Dipartimento di Scienze della Terra, delle Risorse e dell'Ambiente, Università degli Studi di Napoli Federico II, Naples, Italy
10 Department of Earth Sciences, Royal Holloway, University of London, Egham, UK
11 Laboratoire de Sciences du Climat et de l'Environnement, UMR 8212, CEA-UVSQ, IPSL and Université de Paris-Saclay, Gif-sur-Yvette, France
12 Université Paris-Saclay, CNRS, UMR 8148 GEOPS, Orsay, 91405, France
13 Dipartimento di Scienze della Terra e Geoambientali, Aldo Moro-University of Bari, Bari, Italy
14 Dipartimento di Scienze della Terra, Università di Pisa, Pisa, Italy

ABSTRACT

Explosive activity preceding the ~40 ka Campanian Ignimbrite (CI) eruption in the Neapolitan volcanic area, Southern Italy, has long been speculated based on the occurrences of widespread tephra layers, with a Campanian geochemical signature, such as the C-22, X-5, and X-6, preserved in Mediterranean Marine Isotope Stage (MIS) 5 sedimentary records. However, previous studies of pre-CI pyroclastic units occurring in close proximity of the Neapolitan volcanoes, including Campi Flegrei, Somma-Vesuvius, Ischia and Procida islands, did not allow a conclusive identification of the near-source equivalents of these tephra markers. Here we present a comprehensive characterisation of four pyroclastic units from the Campanian Plain, comprising major and trace element glass compositions, Sr-Nd isotopes and $^{40}Ar/^{39}Ar$ dating. Our data allowed the identification of the medial equivalents of the MIS 5 tephra markers, including the widespread C-22, X-5, and X-6 tephra, and their assignment to previously undocumented Campi Flegrei activity between 109-92 ka. In addition to substantially extending Campi Flegrei explosive activity deeper in time, and thus providing the basis for a revaluation of its history, our findings provide new precise radioisotopic dating to better constrain the chronology of the millennial scale climatic oscillations of the MIS 5c-d in the Mediterranean area and possibly on a larger scale.

1. Introduction

Near-vent volcanic successions provide fundamental information for reconstructing the eruption history and dynamics of volcanoes. Proximal exposures, however, often give only fragmentary records of the past activity of a volcanic system, since deposits of older explosive events can be eroded, not preserved or, more commonly, covered by products of younger eruptions. In contrast, tephra layers preserved in sedimentary successions located far away from the volcanic source and characterised by a continuous sediment accumulation history, can provide detailed and undisturbed records of explosive eruptions for a given volcano, including events that are poorly represented or missing in near-vent sections (e.g., Paterne et al., 1988; Monaco et al., 2021).

This could apply to the Neapolitan volcanic area (Campania, southern Italy), including Campi Flegrei, Ischia, Procida and Somma-Vesuvius (Fig. 1b), where the intense Late Pleistocene explosive activity (e.g., Peccerillo, 2017 and reference therein) made the earliest products barely accessible in proximal settings. However, these activities are instead documented in distal sedimentary archives. Indeed, since the first discoveries of Keller et al. (1978), several occurrences of widespread tephra layers with a Campanian geochemical signature embedded within Marine Isotope Stage 5 (MIS 5) sedimentary successions suggested the occurrence of a major explosive activity that, however, had never been documented in proximal sections of the Neapolitan volcanoes. Among them, the C-22 (Paterne et al., 1986), X-5 and X-6 (Keller et al., 1978) tephra layers have been traced widely across the central Mediterranean area in several terrestrial (e.g., Wulf et al., 2004, 2008, 2012, 2018; Marciano et al., 2008; Sulpizio et al., 2010; Giaccio et al., 2012, 2017a; Lucchi et al., 2013; Regattieri et al., 2015; Donato et al., 2016; Leicher et al., 2016; Zanchetta et al., 2018; Petrosino et al., 2019) and marine (e.g., Paterne et al., 1986, 1988, 2008; Bourne et al., 2010, 2015; Insinga et al., 2014; Iorio et al., 2014; Petrosino et al., 2016) sedimentary archives. Moreover, at least two additional tephra, occurring between the C-22 and X5 markers, with a similar Neapolitan geochemical signature, are also found in Mediterranean MIS 5 records (Giaccio et al., 2012, 2017a; Wulf et al., 2012; Leicher et al., 2016; Petrosino et al., 2016).

Over the last decades, these widespread tephra layers have been used as remarkable marker horizons for dating, synchronizing, and correlating the MIS 5 Mediterranean sedimentary successions, the chronologies of which would have otherwise been poorly determined. With this regard, tephra markers from Neapolitan volcanoes arise as pivotal stratigraphic and chronological tools for paleoclimatic and archaeological investigations at the regional scale (e.g., Wulf et al., 2012, 2018; Bourne et al., 2015; Regattieri et al., 2015; Leicher et al., 2016; Petrosino et al., 2016; Giaccio et al., 2017a; Zanchetta et al., 2018).

Despite their great chronological importance, the lack of near-vent counterparts has left the specific volcanic source of these marker layers still undetermined, leading authors to ascribe them either to an unspecified Campanian volcanism (e.g., Wulf et al., 2018), or to an undefined Neapolitan volcanic area (e.g., Giaccio et al., 2017a) or to the so-called “Campanian Volcanic Zone” (CVZ; Rolandi et al., 2003) (e.g., Munno and Petrosino, 2007). Furthermore, in terms of tephrochronological applications, precise and accurate radioisotopic ages are currently available only for two of these markers (i.e., X-5 and X-6), and their full geochemical characterization (i.e., major, trace elements, and Sr-Nd composition) in near-vent outcrops is still pending. Such remaining uncertainties on their origins and incompleteness of their geochronological and geochemical characterization, prevent their use for any volcanological purposes and limit their tephrochronological potential. In order to fill the knowledge gap about these tephra markers and exploit their full potential for both volcanological and tephrochronological perspectives, we acquired stratigraphic, geochemical, and geochronological data for five medial (30-60 km from the vent) pyroclastic units, preceding the Campanian Ignimbrite (CI) eruption, outcropping around the eastern rim of the Campanian Plain (Fig. 1b). Four of these units (Maddaloni, Montemaoro, Cancello and Santa Lucia; Fig. 1b) were previously described (Di Vito et al., 2008), while a fifth one (i.e., Triflisco) is recognised as a distinct, younger event in this study (Fig. 1b). The new chemical, isotopic and geochronological data acquired in this study allowed confidently to correlate the five medial fall units to the widespread X-6, X-5, TM-24b/POP-2a, TM-24a/POP2 and C-22 marker tephra, attributing them to the 109-92 ka Campi Flegrei explosive activity. Our findings thus extend back in time the explosive history of the Campi Flegrei volcanic field and provide new precise dating for refining the chronology of the millennial-scale climatic oscillations of the MIS 5c-d in the Mediterranean area.

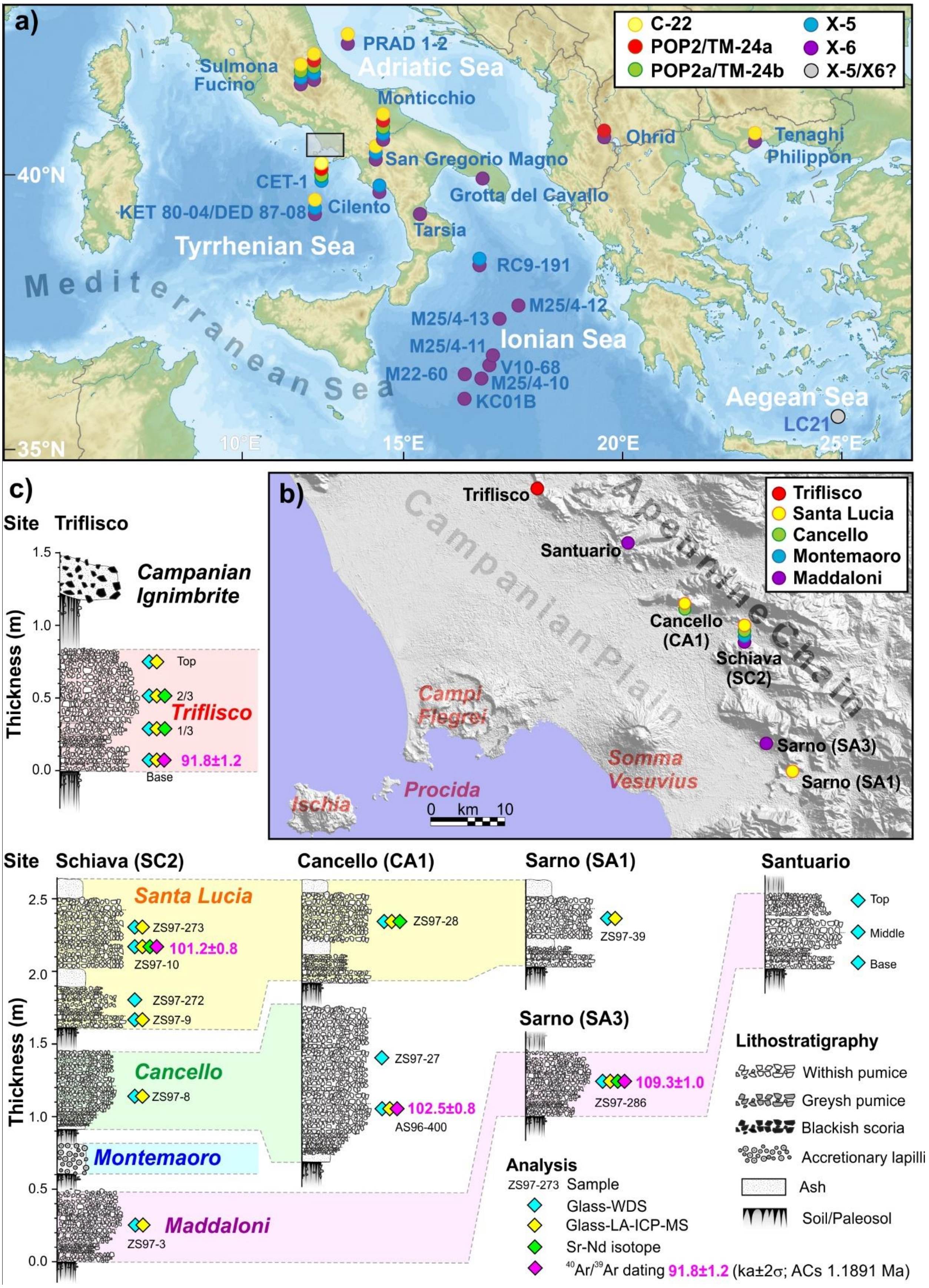

Figure 1. Reference maps and stratigraphic logs of the investigated sections. a) Central Mediterranean sedimentary successions containing the MIS 5 tephra markers investigated in this study. b) Digital Elevation Map (DEM) of the Campanian Plain with location of the Neapolitan volcanoes and the investigated pyroclastic successions (Cancello-SEMAC Quarry, CA1; Schiava-Masseria Montemaoro Quarry, SC2; Sarno-Tre Valloni, SA1; Sarno-Pian della Colla, SA3). c) Stratigraphic logs of the investigated pyroclastic units showing the distribution of the analysed samples and the type of the performed analysis.

2. Geological setting: The Neapolitan volcanoes

The Neapolitan volcanoes comprise Campi Flegrei, Ischia and Procida islands and Somma-Vesuvius (Fig. 1). The Campi Flegrei volcanic field was the site of the most intense activity among the four Neapolitan volcanoes, as well as in the whole Mediterranean area. Three main eruptions occurred in this volcanic area, i.e., the Campanian Ignimbrite (CI; 39.85 ± 0.14 ka; Giaccio et al., 2017b), the Masseria del Monte Tuff (MdMT; 29.3 ± 0.7 ka; Albert et al., 2015, 2019), and the Neapolitan Yellow Tuff (NYT; 14.5 ± 0.4 ka; Deino et al., 2004; Galli et al., 2017) caldera-forming eruptions. Overall, while there is quite satisfactory knowledge on the activity occurred in-between and after these three main events, especially that following the NYT (e.g., Smith et al., 2011), the eruptive history preceding the CI is still poorly resolved, being documented only by deposits sporadically exposed outside the caldera and dated back to ~80 ka (e.g., Pappalardo et al., 1999; Scarpati et al., 2013). Far from the Campi Flegrei volcanic area, several pyroclastic units documenting explosive activity in the Campania region can be dated as back as 290 ka (De Vivo et al., 2001; Rolandi et al., 2003). This older activity is however referred to the so-called Campanian Volcanic Zone (Rolandi et al., 2003), i.e., a hypothesized diffuse, regional volcanism not related to the present Campi Flegrei source area.

Volcanic activity at Ischia Island, off the Naples gulf (Fig. 1b), is documented as back as 150 ka, which is the age of the oldest exposed deposits, and up to historical times (e.g., Poli et al., 1987). The activity of Ischia is subdivided in five stages (i.e., >150-75 ka; 75-55 ka; 55-33 ka; 28-12 ka; 12 ka-1302 CE), characterised by different eruptive styles and types of products (e.g., Poli et al., 1987; Brown et al., 2008). The third stage of activity (55-33 ka) included several explosive events, following the largest 55 ka Monte Epomeo Green Tuff eruption (MEGT; Poli et al., 1987), recognized in the Mediterranean region as the Y-7 tephra marker horizon (e.g., Tomlinson et al., 2014), although this attribution has been recently questioned (D’Antonio et al., 2021).

The Island of Procida, located between Ischia Island and Campi Flegrei (Fig. 1b), was active over a period of ~60 kyr, between ~80 ka and 23,624 ± 330 cal yr BP (e.g., De Astis et al., 2004; Morabito et al., 2014). Its activity originated from five eruptove centres, i.e, Vivara, Terra Murata, Pozzo Vecchio, Fiumicello, and Solchiaro (Rosi et al., 1988a, 1988b) and is documented by pyroclastic deposits and lava dome interbedded with Campi Flegrei and Ischia units, which acts as stratigraphic, chronological markers (e.g., Morabito et al., 2014).

The Somma-Vesuvius stratovolcano, east from the Naples metropolitan area (Fig. 1b), has completely grown on the products of the CI eruption (e.g., Santacroce and Sbrana, 2003), and thus it is younger than 40 ka. Its activity is subdivided in three main stages: (i) the pre-Mercato eruption stage (ca. 35-9 ka), (ii) the stage between Mercato and the infamous AD 79 Pompeii eruption (ca. 9 ka-79 CE) and (iii) the stage following the

Pompeii eruption until present (i.e., last historical eruption of 1944 CE). These three stages differ from one another in terms of either the frequency of the related inter-Plinian eruptive episodes (e.g., Andronico and Cioni, 2002) or the silica undersaturation degree, both increasing over the time (Santacroce et al., 2008).

3. Methods

3.1. Sample selection

For the present study, we used samples collected from 4 eruptive units out of the 14 pre-CI eruption deposits recognised by Di Vito et al. (2008) in the Campanian Plain (Fig. 1b). They are, from bottom to top, SC2-a (hereafter Maddaloni), SC2-b (hereafter Montemaoro), CA1-a (hereafter Cancello), and Santa Lucia (Table 1; Fig. 1c). However, new analysis for Montemaoro unit was not possible due to unavailability of the sample previously collected by Di Vito et al. (2008) and the inaccessibility of the outcrop during the new field investigations. The list of the investigated units is integrated with the fall deposit outcropping near the Triflisco village, at the edge of the Campanian Plain, here labelled Triflisco (Fig. 1b-c). Moreover, the isotopic characterisation has been performed also on samples CIL1 and CIL2 from the Cilento Coast being representative of the X5 and X6 stratigraphic markers (Giaccio et al. 2012).

Table 1. Location and data summary of the investigated units.

Units	Locality	Sample source	Coordinates	Sample/sub-units	Analysis			
					Major elements (EMPA)	Trace elements (LA-ICP-MS)	Sr-Nd isotopes	$^{40}Ar/^{39}Ar$ age
Triflisco	Triflisco	This study	41°08’14’’ N 14°15’12’’ E	TRIF-Top	Y	Y	-	-
				TRIF-2/3	Y	Y	Y	-
				TRIF-1/3	Y	Y	Y	-
				TRIF-Base	Y	Y	-	Y
Santa Lucia (Santa Lucia)	Schiava, Masseria Montemaoro Quarry (SC2)	Di Vito et al. (2008)	40°56’39’’ N 14°33’56’’ E	ZS97-9	Y	Y	-	-
				ZS97-10	Y	Y	Y	Y
				ZS97-272	Y	Y	-	-
				ZS97-273	Y	Y	-	-
	Cancello, SEMAC Quarry (CA1)		40°59’11’’ N 14°29’27’’ E	ZS97-28	Y	Y	Y	-
	Sarno, Tre Valloni (SA1)		40°49’03’’ N 14°38’06’’ E	ZS97-39	Y	Y	-	-
Cancello (CA1-a)	Cancello, SEMAC Quarry (CA1)	Di Vito et al. (2008)	40°59’11’’ N 14°29’27’’ E	ZS97-27	Y	-	-	-
				AS96-400	Y	Y	-	Y
	Schiava, Masseria Montemaoro Quarry (SC2)		40°56’39’’ N 14°33’56’’ E	ZS97-8	Y	Y	-	-
Montemaoro (SC2-b)	Schiava, Masseria Montemaoro-Quarry (SC2)	Di Vito et al. (2008)	40°56’39’’ N 14°33’56’’ E	SC2-b	-	-	-	-
Maddaloni (SC2-a)	Santuario di San Salvatore	This study	41°03’11’’ N 14°23’47’’ E	Top	Y	-	-	-
				Middle	Y	-	-	-
				Base	Y	-	-	-
	Schiava, Masseria Montemaoro-Quarry (SC2)	Di Vito et al. (2008)	40°56’39’’ N 14°33’56’’ E	ZS97-3	Y	Y	-	-
	Sarno, Pian della Colla (SA3)		40°48’44’’ N 14°39’31’’ E	ZS97-286	Y	Y	Y	Y
CIL1	Cilento Cost	Giaccio et al. (2012)	40°03’24’’N 15°17’02’’E	CIL1	Y[1]	-	Y	-
CIL2				CIL2	Y[1]	-	Y	-

"Y": type of analysis performed on the sample. "-": type analysis not performed on the sample. Literature data source: [1] = Giaccio et al. (2012).

3.2. Volcanic glass characterisation

3.2.1. Sample preparation

The samples selected for the major and trace glass composition (Fig. 1c; Table 1) were wet sieved with tap water through a series of sieves with decreasing mesh openings. All fractions were successively oven-dried at 100°C until completely dry. For major element analysis, selected fractions of 60-250 μm were mounted on 29 x 49 mm glass slides, embedded in epoxy resin, progressively ground to a thickness of 60-100 μm and finally polished to be analysed with the electron microprobe. For trace element analysis, selected samples were embedded in epoxy resin and successively polished.

3.2.2. Electron probe micro analyser (EPMA)

Glass shards and (micro-)pumice fragments were analysed by single-shard major element chemical analysis using the electron probe micro analyser (EPMA). Analysis was first performed with a Jeol JXA-850F equipped with five wave dispersive spectrometers (WDS), installed at the Institute of Petrology and Structural Geology, Charles University of Prague (Prague, Czech Republic). The machine operated at 15 kV accelerating voltage, 10 nA beam current and 10 μm defocused beam to limit alkali loss. Element counting times were of 20 s for all elements, except for Na, K, and S, for which counting times of 10 s (Na and K) and 30 s (S) were employed respectively. For all measurements, the F content was always below the detection limit of the machine. Standards for calibration were quartz (Si), corundum (Al), rutile (Ti), magnetite (Fe), periclase (Mg), rhodonite (Mn), albite (Na), sanidine (K), diopside (Ca), apatite (P and F), tugtupite (Cl) and anhydrite (S). The secondary standards GOR128-G (Jochum et al., 2006) and CFA47 (Marianelli and Sbrana, 1998) were analysed at the beginning of each microprobe session for a total of one point each to evaluate analysis accuracy.

Further WDS analyses were carried out at the Dipartimento di Scienze della Terra, Università degli Studi di Firenze (Florence, Italy), with a Jeol Superprobe JXA-8230 equipped with five-WDS spectrometers. Operating conditions were set to 15 kV accelerating voltage, 10 nA beam current and 10 μm defocused beam diameter to limit Na mobilisation. Element counting times were 15 s for all elements except for Na (10s), F (20s), S (30s), Mn, P and Cl (40s). Albite (Si and Na), ilmenite (Ti and Fe), plagioclase (Al), bustamite (Mn), olivine (Mg), diopside (Ca), sanidine (K), apatite (P), fluorite (F), tugtupite (Cl) and celestine (S) were used as internal standards. The accuracy of the measurements was assessed using the glass secondary standards GOR128-

G, ATHO-G and StHs6/80-G (Jochum et al., 2006), Lipari ID3506 (Kuehn et al., 2011), Scapolite NMNH, and CFA47 (Marianelli and Sbrana, 1998).

For both analytical facilities, the ZAF method was used for matrix effect correction. We adopted 93 wt% as a threshold for the measured totals. All compositional data are shown as oxide weight percentages (wt%) in the TAS and bi-plots diagrams, with total iron measured as FeO, and normalised to 100% on a volatile-free basis for correlation purposes. Collected data and secondary standards measurements are all reported in Supplementary Materials-1.

3.2.3. Laser Ablation Inductively Coupled Plasma Mass Spectrometry (LA-ICP-MS)

Trace element analyses were conducted on volcanic glasses from the Triflisco, Santa Lucia, Cancello, and Maddaloni units. The analyses were performed using an Agilent 8900 triple quadrupole ICP-MS (ICP-QQQ) coupled to a Resonetics 193nm ArF excimer laser-ablation device at the Department of Earth Sciences, Royal Holloway, University of London. Full analytical procedures used for volcanic glass analysis follow those reported in Tomlinson et al. (2010). Crater sizes of 20, 25 and 34 µm were used depending on the sample vesicularity and/or size of glass surfaces available for analysis. The repetition rate was 5 Hz, with a count time of 40 s on the sample, and 40 s on the gas blank to allow the subtraction of the background signal. Typically, blocks of eight glass shards and one MPI-DING reference glass were bracketed by the NIST612 glass adopted as the calibration standard. The internal standard applied was ^{29}Si (determined by EMP-WDS analysis). In addition, MPI-DING reference glasses were used to monitor analytical accuracy (Jochum et al., 2006). LA-ICP-MS data reduction was performed in Microsoft Excel, as outlined in Tomlinson et al. (2010). Accuracies of LA-ICP-MS analyses of the MPI-DING reference glasses, ATHO-G and StHs6/80-G, were typically ≤ 5% for the majority of elements measured. Tephra and standard measurements are all provided in Supplementary Materials-1. Data averages reported in the text are accompanied by a ± 2 standard deviation (2 s.d.), whilst error bars in the plots are typically smaller than the data symbols.

3.2.4. Sr and Nd isotopes

$^{87}Sr/^{86}Sr$ and $^{143}Nd/^{144}Nd$ isotope ratios have been determined on two samples from the Santa Lucia and one from Maddaloni units (i.e., ZS97-10 and ZS97-28, and ZS97-286 respectively) previously investigated by Di Vito et al. (2008), on two samples from the Triflisco unit (i.e., TRIF 1/3 and TRIF 2/3) and on the CIL1 and CIL2 units from the Cilento Coast (Giaccio et al. 2012; Fig. 1c; Table 1). Measurements have been performed either on the glasses (pumices) and/or crystals (pyroxene or feldspar). $^{143}Nd/^{144}Nd$ measurement were performed on the glass fraction of samples from Triflisco, Santa Lucia (ZS97-10) and Maddaloni (ZS97-286) units. The different fractions were handpicked under a binocular microscope. Among all the available glass shards/pumices the most homogeneous in colour, and visibly poorly affected by secondary alteration, were selected for isotope analyses. Feldspar and pyroxene crystals were handpicked avoiding those characterised by the presence of glass rinds attached on their surfaces.

Before chemical dissolution, glass shards/pumices were acid leached three to five times to reduce as much as possible the alteration effects. The leaching procedure was prolonged until the acid solution became light-yellow in colour. Leaching was carried out each time by placing the beakers containing samples and high purity 6N HCl on a hot plate for 10 min. During each leaching step and after the final leaching, samples were rinsed with Milli-Q® H_2O. Feldspar and pyroxene were cleaned with Milli-Q® H_2O for 10 min. in an ultrasonic bath. Dissolution was obtained with high-purity HF–HNO_3–HCl mixtures. Sr and Nd were separated from the matrix through conventional ion-exchange procedures. Sr and Nd isotopic compositions were determined in a static mode by thermal ionisation mass spectrometry (TIMS) using a Thermo Finnigan Triton TI® mass spectrometer equipped with one fixed and six adjustable Faraday cups. Average 2σ mean, i.e., the standard error with N = 180, was better than ± 9×10^{-6} for Sr, and better than ± 7×10^{-6} for Nd measurements. The mean measured values of $^{87}Sr/^{86}Sr$ for the NIST-SRM 987 standard and $^{143}Nd/^{144}Nd$ for the La Jolla standard were 0.710261 ± 0.000021 (2σ, N = 169) and 0.511845 ± 0.000010 (2σ, N = 55), respectively; external reproducibility (2σ) during the period of measurements was calculated according to Goldstein et al. (2003). Measured $^{87}Sr/^{86}Sr$ ratios were normalized for within-run isotopic fractionation to $^{86}Sr/^{88}Sr$ = 0.1194, and $^{146}Nd/^{144}Nd$ = 0.7219. The final, measured isotope ratio values were normalized to the recommended values of the NIST SRM 987 ($^{87}Sr/^{86}Sr$ =0.71025) and La Jolla ($^{143}Nd/^{144}Nd$ = 0.51185) standards, respectively. Chemistry processing and isotope analyses were performed at the Radiogenic Isotope Laboratory (RIL) of the Istituto Nazionale di Geofisica e Vulcanologia, Osservatorio Vesuviano, and the full analytical dataset is reported in Supplementary Materials-2.

3.2.5. $^{40}Ar/^{39}Ar$ dating

The $^{40}Ar/^{39}Ar$ ages were obtained at the Laboratoire des Sciences du Climat et de l’Environnement (CEA, CNRS UMR 8212, Gif-sur-Yvette, France) dating facility. Fresh and transparent K-rich feldspars were extracted from Triflisco, Santa Lucia, Cancello and Maddaloni samples. After being washed in distilled water, transparent K-feldspars (500-630 μm) without any visible inclusions were handpicked under a binocular and used for dating these four pyroclastic units.

Between 20 and 30 crystals for each sample were irradiated in the Cd-lined, in core CLICIT facility of the Oregon State University TRIGA reactor for 2 h (IRR. CO-007) for Triflisco and 1 h in the same reactor (IRR. CO-009) for Santa Lucia, Cancello, and Maddaloni. Interference corrections were based on the nucleogenic production ratios given in Balbas et al. (2016). After irradiation, individual crystal for each tephra layers were transferred into a copper 133 pits sample holder placed into a differential vacuum Teledyne Cetac window connected to a home designed compact extraction line. Minerals were fused one by one using a 100W Teledyne Cetac CO_2 laser during 15s at 2.5 W. Before fusion, each crystal underwent a 10s long sweeping at 0.3W to remove unwanted gas potentially trapped on the crystals surface and fractures. Extracted gases were firstly purified by a SAES GP 50 cold getter for 90s and then for 230s by two hot SAES GP 50 getters. The five Argon isotopes (i.e., ^{40}Ar, ^{39}Ar, ^{38}Ar, ^{37}Ar and ^{36}Ar) were measured using a multicollector NGX 600 mass spectrometer equipped with 9 ATONA® amplifiers array and an electron multiplier. More technical specifications regarding the NGX 600 ATONA detector array are presented in detail in Cox et al. (2020). ^{40}Ar, ^{39}Ar, ^{38}Ar, and ^{36}Ar isotopes were collected simultaneously while the ^{37}Ar was measured in a second time. In the first run, ^{40}Ar, ^{39}Ar and ^{38}Ar were measured simultaneously on 3 ATONA® amplifiers and ^{36}Ar on the electron multiplier. Following this first run the ^{37}Ar was measured alone using the electron multiplier. Each isotope measurement corresponds to 15 cycles of 20-seconds integration time. Peak intensity data were reduced using ArArCALC V2.4 (Koppers, 2002). Neutron fluence J factor was calculated using co-irradiated Alder Creek sanidine standard ACs-2 associated to an age of 1.1891 Ma (Niespolo et al., 2017) according to the K total decay constant of Renne et al. (2011) ($\lambda_{e.c.} = (0.5757 \pm 0.016) \times 10^{-10}$ yr^{-1} and $\lambda_{\beta^-} = (4.9548 \pm 0.013) \times 10^{-10}$ yr^{-1}). To determine the neutron flux for each sample we used at least 6 flux monitor crystals coming from pits framing the samples in each irradiation disk. J-values are of 0.00056080 ± 0.00000062 (Triflisco [Base]); 0.00028350 ± 0.00000023 (Santa Lucia [ZS97-10); 0.00028340 ± 0.00000028 (Cancello [AS96-400]); 0.00028340 ± 0.00000020 (Maddaloni [ZS97-286]). To verify the detectors linearity, mass discrimination was monitored by analysis of at least 60 air shots of various beam sizes ranging from 5.0 10^{-3} up to 2.0 10^{-2} V (1 to 4 air shots). About 15 air shots analyses are performed every day. These measurements are done automatically during the nights before and after the unknown measurements. Discrimination is calculated according the $^{40}Ar/^{36}Ar$ ratio of 298.56 (Lee et al., 2006). Procedural blank measurements were achieved after every two to three unknowns. For typical 5 min time blank backgrounds are between 2.5 and 4.0 10^{-4} V for ^{40}Ar and 60 to 90 cps for ^{36}Ar (about 1.0-1.3 10^{-6} V equivalent). Full analytical data for each sample can be found in Supplementary Materials-3.

4. Results

4.2. Stratigraphy

Most samples investigated in this study refer to the pyroclastic units already described in Di Vito et al. (2008), to which the reader is referred for the lithostratigraphic details. They generally consist in dm-thick fallout deposits made up of either pumice lapilli or coarse ash (Fig. 1c). At the site "Schiava" (SC2 in Fig. 1b) all the four previously investigated units, i.e., Maddaloni, Montemaoro, Cancello and Santa Lucia, occur as distinct eruptive units separated by either paleosols, epiclastic deposits or unconformity bounding surfaces.

The newly recognised Triflisco unit (Fig. 1b), consists in an 80 cm-thick fallout deposit made up of moderately sorted, white-pinkish and well-vesicular pumice lapilli (max Φ 3 cm) with intervening coarse ash layers. Accidental lithics are scant (Fig. 1c). The Triflisco unit overlies a paleosol and at the top, in turn, it is capped by a thick reddish paleosol on which lays a greyish pyroclastic flow deposit that we attribute to the CI (Fig. 1c). Thus, our interpretation differs from previous ones that correlated the pumice fall at this locality to the CI Plinian fall exposed elsewhere (Civetta et al., 1997; Fanara et al., 2015).

The Maddaloni unit was also sampled in a new exposure at Santuario di San Salvatore (Fig. 1b), where it consists in a 50 cm-thick fallout deposit made up of well sorted, white-greyish sanidine-bearing and highly vesicular pumiceous lapilli (max Φ 4-5 cm), with highly elongated bubbles, containing scant accidental lithics (Fig. 1c). At this site, the Maddaloni unit overlies a paleosol, whereas its uppermost part is not exposed, because of the vegetation cover.

4.3. Major and minor element volcanic glass chemistry

All samples analysed in this study have a dominant composition overlapping the boundary between phonolite and trachyte fields (Fig. 2a) of the *Total alkali vs Silica* (TAS, Le Maitre et al., 2002) classification diagram. Mean compositions are reported at 2 σ (2 standard deviation) error.

Triflisco unit. It is made up by four sub-units (Fig. 1c) with a relatively homogeneous composition. The majority of the data straddle the boundary between trachyte and phonolite fields (SiO_2 content of 59.5 ± 0.9 wt%, and alkali sum of 12.8 ± 1.0 wt%), depicting a trend within the trachyte field with decreasing alkali negatively correlated with a small increase in silica; Fig. 2a-b). The CaO/FeO values are < 1 (0.8 ± 0.1) and the Cl content is 0.6 ± 0.1 wt% for all sub-units (Fig. 2c). Glasses display a High Alkali Ratio (HAR), with K_2O/Na_2O generally > 2 and up to 3.08 (Fig. 2d). There is no appreciable chemical variation from the lowermost (Triflisco Base) to the uppermost (Triflisco Top) sub-units.

Santa Lucia unit. The glass of this unit, analysed in six samples (Fig. 1c; Table 1), is characterised by the most heterogeneous composition among those analysed, although mainly phonolitic, with a mean SiO_2 content of 59.0 ± 2 wt%, and an alkali sum of 12.8 ± 1 wt% (Fig. 2a-b). The CaO/FeO ratio is ≤ 1 (mean of 0.9 ± 0.1) and the Cl content is medium-high (0.6 ± 0.1 wt%; Fig. 2c). Santa Lucia glasses display a HAR typically ≥ 2, with a mean K_2O/Na_2O ratio of 2.1 ± 0.5 (Fig. 2d).

Cancello unit. Glasses from this unit are phonolitic-trachytic in composition, with a SiO_2 content of 60.9 ± 1.3 wt%, a mean alkali sum of 13.1 ± 0.9 wt% (Fig. 2a-b) and a HAR of 2.2 ± 0.6 (Fig. 2d). The CaO/FeO ratio ranges between 0.7 and 1.0 and the Cl content between 0.5 and 0.7 wt% (Fig. 2c).

Montemaoro unit. As stated in the previous section, it was not possible to acquire new data for this unit. Thus, for the purpose of this study, we rely on the available glass-EDS data from Di Vito et al. (2008). The Montemaoro unit is mainly trachytic in composition with some points straddling the boundary with the phonolite field, with silica and alkali sum content of c.a. 61 wt% and 13 wt%, respectively (Fig. 2a-b). The glasses display a HAR, up to 2.5, with a CaO/FeO ratio of c.a. 0.7 (Fig. 2d), while Cl content was not determined.

Maddaloni unit. The glass of this unit, collected from the former SC2 and SA3 sections and the new Santuario one (Fig. 1; Table 1), is characterised by a homogeneous SiO_2 content (mean 61.6 ± 0.8 wt%), with an alkali sum of 13.8 ± 0.5 wt% (Fig. 2a-b). Respect to all the above-mentioned samples, Maddaloni glasses predominantly display a Low Alkali Ratio (LAR), with K_2O/Na_2O typically ≤ 1.5 (1 ± 0.3; Fig. 2d), due to an almost equal content of K_2O and Na_2O of ca. 7 wt%. In addition to a lower K_2O/Na_2O ratio, with respect to the other analysed units, the glass of the Maddaloni pumices has noticeably lower CaO/FeO ratios (0.6 ± 0.1), whilst the Cl content is appreciably higher, up to 1.1 wt% (Fig. 2c).

4.4. Trace element volcanic glass chemistry

The Triflisco eruption unit contains HAR glasses that are fairly homogeneous in terms of their incompatible trace element contents (e.g., Th = 29.9 ± 2.9 ppm [Fig. 2e-f]; Nb = 59.2 ± 4.0 ppm [Fig. 2e]; Zr = 327 ± 31 ppm [Fig. 2f]) and ratios of other High Field Strength elements (HFSE) to Th remaining constant (e.g., Nb/Th = 2.0 ± 0.1; Zr/Th = 10.9 ± 0.5). Light Rare Earth Elements (LREE) are enriched relatively to the Heavy Rare Earth Elements (HREE) with La/Yb = 27.9 ± 3.7.

The HAR Santa Lucia eruption products in the SC2, CA1 and SA1 sections (see Table 1) are compositionally consistent and fairly homogeneous (e.g., Th = 27.1 ± 3.1 ppm; Nb = 55.8 ± 4.5 ppm [Fig. 2e]; Zr = 306 ± 29 ppm [Fig. 2f]; Rb = 307 ± 25 ppm; La = 77.9 ± 6.0 ppm) with constant HFSE/Th ratios (Nb/Th = 2.1 ± 0.1; Zr/Th = 11.3 ± 0.5) and displaying LREE enrichment relatively to HREE (La/Yb = 27.7 ± 3.1).

The Cancello unit displays HAR glasses that are fairly homogeneous in composition (e.g., Th = 26.7 ± 3.0 ppm; Nb = 56.1 ± 7.0 ppm [Fig. 2e]; Zr = 316 ± 34 ppm [Fig. 2f]; La = 81.4 ± 8.3 ppm), with minor variation relating to a single less enriched analysis. HFSE to Th ratios remain constant within the Cancello glasses (Nb/Th = 2.1 ± 0.2; Zr/Th = 11.8 ± 0.4), and LREE are enriched relative to the HREE where La/Yb = 27.6 ± 3.4.

The LAR Maddaloni tephra shows variable incompatible trace element glasses compositions (e.g., Th = 84-114 ppm; Nb = 169-231 ppm [Fig. 2e]; Zr = 1037-1319 ppm [Fig. 2f]) and displays far greater levels of enrichment relative to the above mentioned HAR units (i.e., Triflisco, Santa Lucia and Cancello; Fig. 2e-f). HFSE/Th values remain constant within these glasses (Nb/Th = 2.1 ± 0.1; Zr/Th = 11.8 ± 0.4) and are entirely consistent with the HAR samples from Triflisco, Santa Lucia and Cancello deposits (Fig. 2e-f).

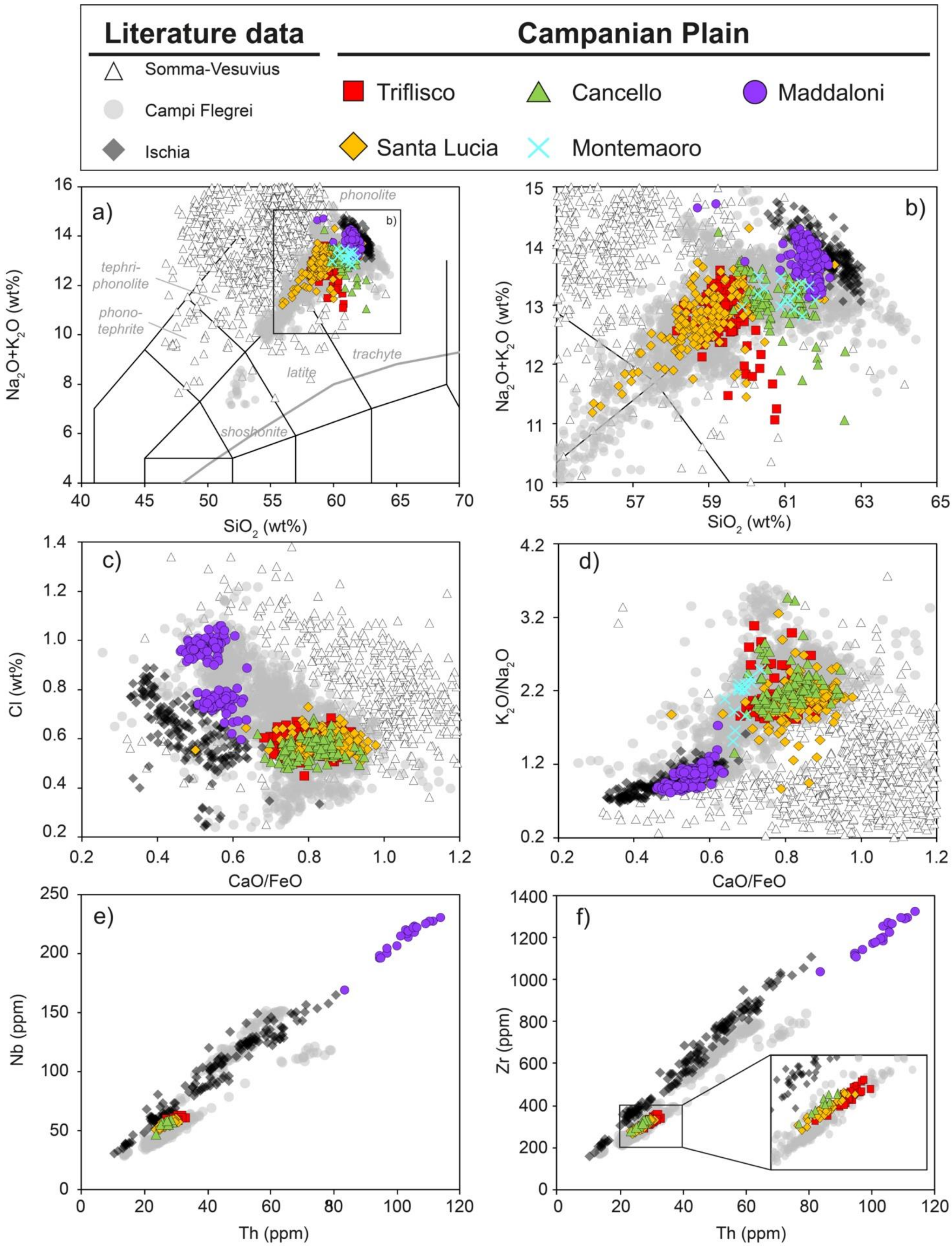

Figure. 2. Major and trace element compositions of the investigated medial Campanian Plain units in comparison with literature data of Ischia and Campi Flegrei volcanic systems. (a, b) *Total alkali vs silica* (TAS; Le Maitre et al., 2002), (c) CaO/FeO vs Cl classification diagram (Giaccio et al., 2017a), (d) CaO/FeO vs K_2O/Na_2O, (e) Th vs Nb (ppm) and (f) Th vs Zr (ppm). Glass-WDS data source: Triflisco, Santa Lucia, Cancello and Maddaloni medial Campanian Plain units: this study; Somma-Vesuvius: Santacroce et al. (2008); Ischia: Tomlinson et al. (2014); Campi Flegrei: Smith et al. (2011, 2016), Tomlinson et al. (2012). Trace elements data source: Triflisco, Santa Lucia, Cancello and Maddaloni medial Campanian Plain units: this study; Ischia: Tomlinson et al. (2014); Campi Flegrei (Tomlinson et al., 2012).

4.5. Sr and Nd isotopes

Whilst the ^{143}Nd/^{144}Nd isotopic ratios are homogeneous within the analytical error (c.a. 0.51250), the ^{87}Sr/^{86}Sr ratios (Fig. 3a) range from 0.70687 and 0.70780 (glass from sample ZS97-286). The highest value is possibly due to post-depositional alteration of the glass as suggested by the Sr isotope composition of the embedded feldspar. Samples from Triflisco and Santa Lucia display similar and lower Sr isotope composition (c.a. 0.7069) with respect to sample from Maddaloni unit. CIL1 and CIL2 are characterized by Sr isotope ratios (from ca. 0.7071 to 0.7072) similar to that of the Maddaloni feldspar (from c.a. 0.7071). Figure 3 displays the variations in terms of Sr-Nd isotope ratios compared with literature data.

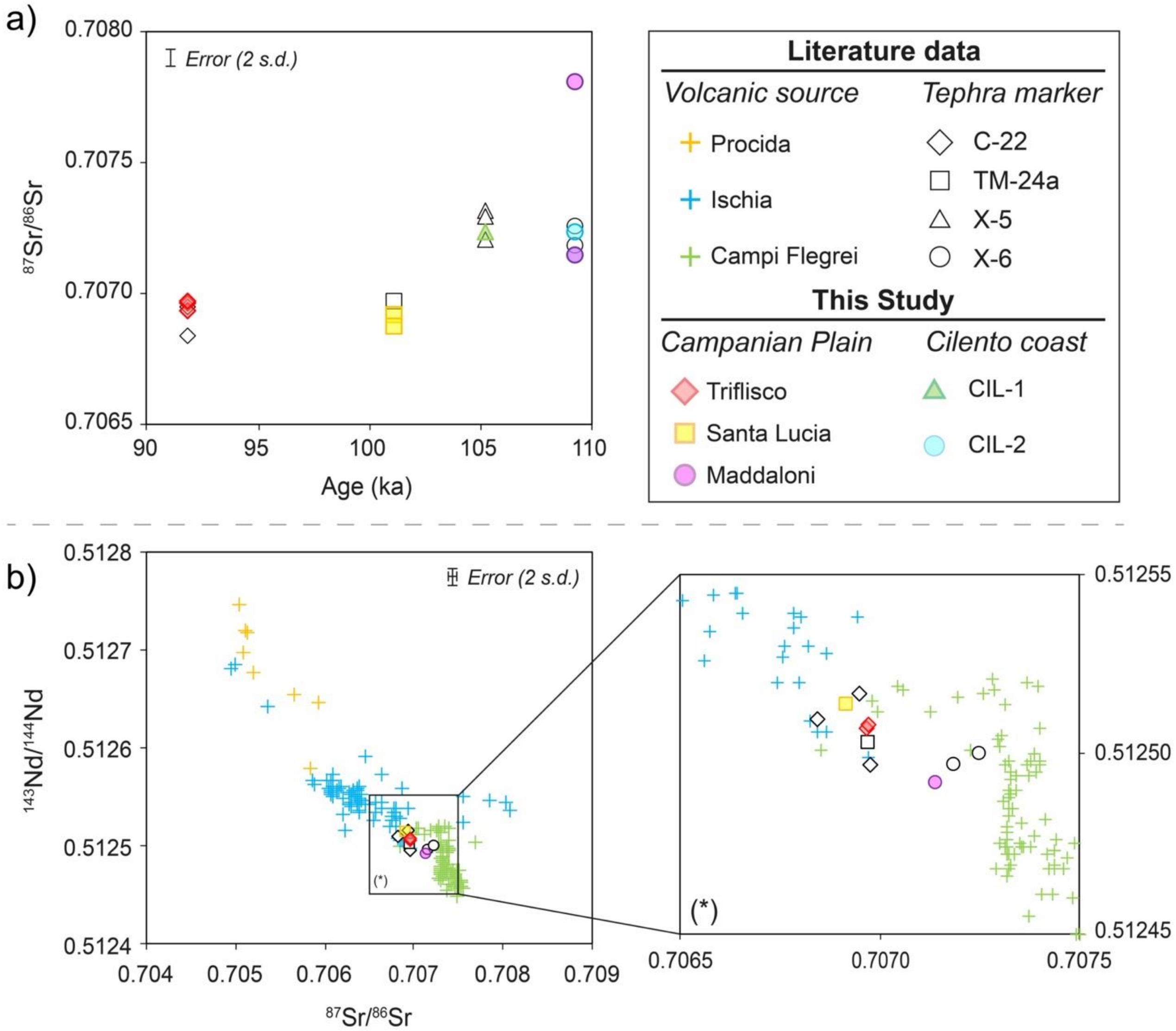

Figure. 3. Sr and Nd isotope ratios determined for the Triflisco, Santa Lucia and Maddaloni units from the Campanian Plain and CIL-1 and CIL-2 tephra from the Cilento coast. In panel b the Sr isotope composition of the feldspar from the Maddaloni sample has been associated to the Nd isotope composition of its glass fraction, being the glass possibly affected by post depositional alteration. This latter did not modify the ^{143}Nd/^{144}Nd, because the Nd is a less fluid mobile element. Tephra layers literature data source: **C-22**: POP-1 (Giaccio et al., 2012), TF-10 (Giaccio et al., 2017a), S14 (Petrosino et al., 2019); **TM-24a:** POP-2A (Giaccio et al., 2012); **X-5**: TF-12 (Giaccio et al., 2017a), S11 (Petrosino et al., 2019); **X-6** = TF-13 (Giaccio et al., 2017a), S10 (Petrosino et al., 2019). Literature data for Ischia, Procida and Campi Flegrei proximal deposits: Arienzo et al. (2009, 2010, 2015, 2016), Brown et al. (2014), Casalini et al. (2018), D'Antonio et al. (2007, 2013), Di Renzo et al. (2011), Pabst et al. (2008), Pelullo et al. (2020), Tonarini et al. (2009).

4.6. $^{40}Ar/^{39}Ar$ ages

All $^{40}Ar/^{39}Ar$ results for individual tephra layers are presented as probability diagrams (Fig. 4). Weighted mean age uncertainties are all reported at 2σ, including J uncertainty and were calculated using Isoplot 4.0 (Ludwig, 2001). For each sample, inverse isochrones have an atmospheric $^{40}Ar/^{36}Ar$ initial intercept with uncertainties suggesting that dated crystals are without detectable excess argon. Full inverse isochrones dataset can be found in Supplementary Materials-3.

Triflisco (TRIF-Base) - 13 single crystals were individually dated. Eleven out of thirteen crystals analysed gave a similar age within uncertainties (Fig. 4a). The two other older crystals, one sanidine and one plagioclase according to their Ca/K ratio, are interpreted as xenocrysts. The main population of crystal interpreted as juvenile allows to calculate a weighted mean age of 91.8 ± 1.2 ka (MSWD = 1.20, p = 0.27).

Santa Lucia (ZS97-10) - A total of 14 individual sanidine crystals were dated. The probability diagram is simple (Fig. 4b) with one mode allowing to calculate a meaningful and precise weighted mean age of 101.2 ± 0.8 ka (MSWD = 0.59, p = 0.87).

Cancello (AS96-400) - The probability diagram displays one single mode with no xenocrystal contamination (Fig. 4c). These crystals are interpreted as juvenile ones (12 crystals), allowing to calculate a precise weighted mean age of 102.5 ± 0.8 ka (MSWD = 0.58, p = 0.85).

Maddaloni (ZS97-286) - 14 crystals were dated individually. All gave within uncertainty the same age resulting in a gaussian probability diagram (Fig. 4d). Using this very homogenous crystal population we calculated a weighted mean age of 109.3 ± 1.0 ka (MSWD = 0.43, p = 0.96).

While for Maddaloni we obtained the $^{40}Ar/^{39}Ar$ age of 109.3 ± 1.0 ka, the overlying Montemaoro unit, which was not resampled or re-analysed in this work, was not dated.

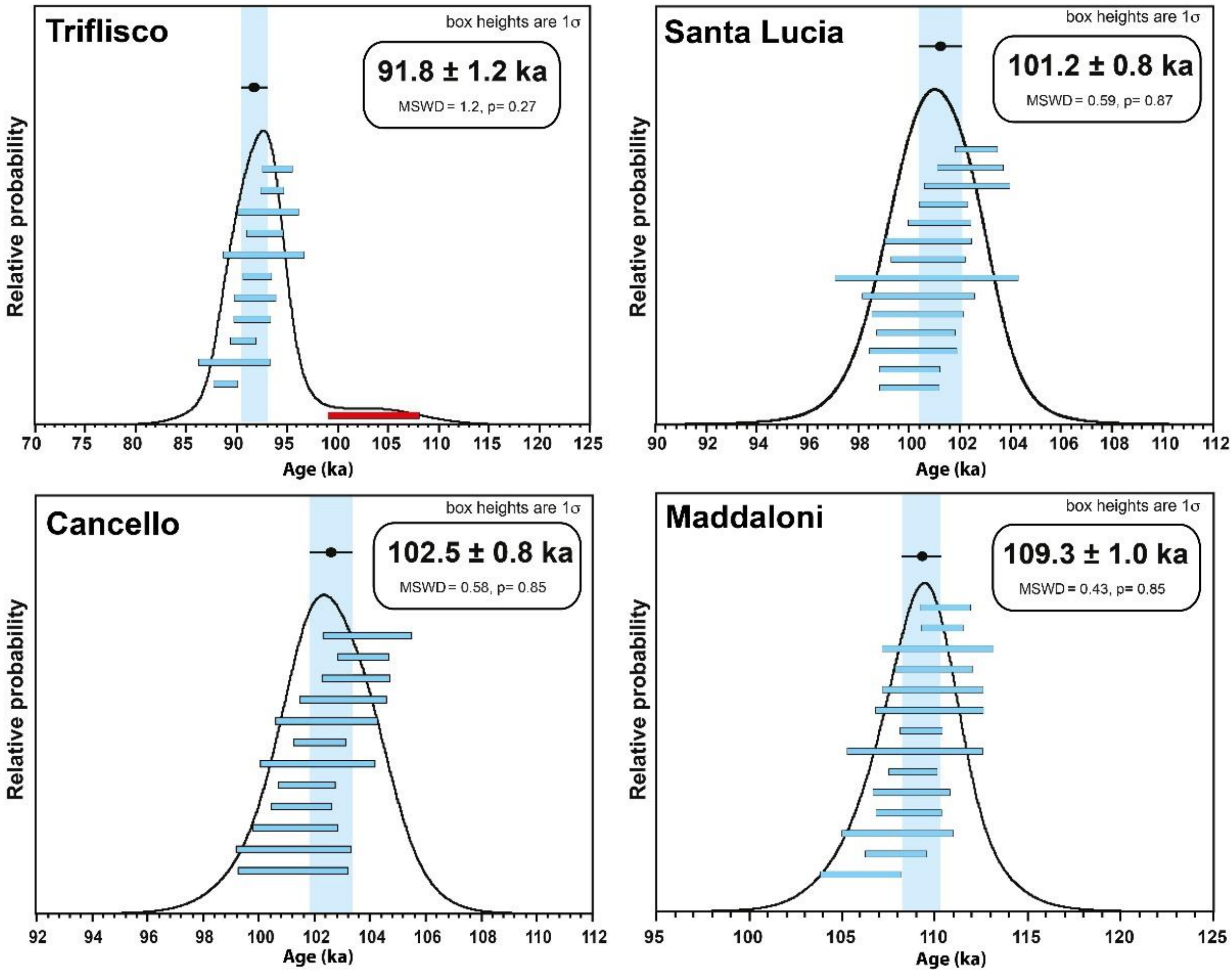

Figure. 4. Age probability diagrams for the Triflisco, Santa Lucia, Cancello and Maddaloni units.

5. Discussion

5.1. Volcanic source of the Campanian Plain Units

All the investigated pyroclastic fall units occur in a range of 30-35 km to 55-60 km in the eastern quadrants from the Neapolitan volcanoes, including Campi Flegrei, Ischia, Procida and Somma-Vesuvius (Fig. 1b). Somma-Vesuvius can be reasonably excluded as a potential source since its oldest known activity is younger than Campanian Ignimbrite (i.e., < 40 ka; Santacroce et al., 2008) and thus incompatible with the 109-92 ka chronology obtained here for the Campanian Plain units. Also, in terms of glass chemical composition, the Somma-Vesuvius products appear incompatible due to the higher alkali sum at similar SiO_2 content (Fig. 2a-b), and the significantly higher CaO/FeO at same Cl content and alkali ratio (Fig. 2c-d). Procida island can also be excluded based on the Sr-Nd isotope compositions, which are clearly different from those of the Campanian Plain units (Fig. 3a-b). Among the two remaining potential sources for the investigated units (i.e., Campi Flegrei and Ischia), based on the lithostratigraphic and geochemical characteristics, as already argued by Di Vito et al. (2008), the Campi Flegrei volcanic area is the most probable. In terms of major element glass composition, although Campi Flegrei and Ischia products partially overlap, each of the two volcanic sources show distinctive features in terms of oxide concentrations and ratios (Fig. 2a-d). This applies to four out of the five investigated units (i.e., Triflisco, Santa Lucia, Cancello, and Montemaoro), which unambiguously plot in the compositional field of the Campi Flegrei glass because of the higher K_2O/Na_2O and CaO/FeO values with respect to the Ischia products (Fig. 2b-c). Trace elements glass compositions also support the attribution of the Triflisco, Santa Lucia and Cancello units to the Campi Flegrei, for instance all these units show enrichment in Zr that is diagnostic of the Campi Flegrei products and is slightly lower than that of the products typically erupted at Ischia (Fig. 2f).

Owing to its distinctive K_2O/Na_2O and CaO/FeO values, which are lower than those of the most common Campi Flegrei products (Fig. 2c-d), the source attribution of the Maddaloni unit is not so straightforward. Indeed, CaO/FeO and K_2O/Na_2O ratios of Maddaloni unit partly overlap with those of Ischia (Fig. 2b-c). However, using the CaO/FeO vs. Cl diagram, the glass composition of Maddaloni unit falls out of the Ischia field and within the Campi Flegrei one, though, sporadically, the Campi Flegrei compositions can overrun the typical Ischia one (Fig. 2c). Indeed, such chemical characteristics, i.e., LAR trachyte-phonolite with relatively low CaO/FeO ratio, are also found in Campi Flegrei products (e.g., Tomlinson et al., 2012), notably in the CI (Smith et al., 2016) and some minor Campi Flegrei eruptions following the NYT caldera-forming eruption (e.g., Averno 2, Fondi di Baia, Monte Nuovo; Smith et al., 2011). Likewise, the Maddaloni unit can be attributed to the Campi Flegrei and ascribed to this less common, LHR trachyte-phonolite compositional group of this volcanic area. Incompatible trace element enrichment of the Maddaloni glasses exceeds that currently recognised in the known products of Campi Flegrei and Ischia (Fig. 2e-f) making their use again less conclusive. However, the lower Zr/Th ratios observed in the Maddaloni glasses are seemingly more akin to those of Campi Flegrei, rather than to the higher values typically observed in the eruptive products of Ischia spanning a period of intense explosive volcanism at ~40-80 ka (Tomlinson et al., 2014). More convincing, and seemingly definitive, evidence to confirm Campi Flegrei as the source for the Maddaloni unit, is provided by isotope data. Indeed, the Sr- and Nd-isotope compositions for the Maddaloni samples are positioned well within the field of the Campi Flegrei (Fig. 3a-b).

In summary, the volcanological and sedimentological constraints, the acquired major and trace elements glass composition, the geochronological and Sr- and Nd-isotope data consistently indicate that Campi Flegrei is the most probable source for all the five investigated Campanian Plain units. This significantly extends back in time the known explosive activity of this volcanic field, previously documented only up to ca. 80 ka (Scarpati et al., 2013), or as far back as 290 ka (CVZ; De Vivo et al., 2001; Rolandi et al., 2003). Regardless the precise vent location, our data point to a frequent activity that took place within the Campi Flegrei volcanic area. Specifically, we recognised five eruptions that, based on their lithological features in medial settings, can be likely considered of Plinian intensity and magnitude. These occurred across approximately a 17 kyr time-window, with recurrence times of a few thousands of years and in one case are barely more than 1 kyr (e.g., time elapsed between the 102.5 ± 0.8 ka Cancello and the 101.2 ± 0.8 ka Santa Lucia eruptions). Consequently, the period of 109-92 ka was characterized by a high frequency of moderate to large explosive eruptions, i.e., an eruptive behaviour that has not been recognised within the more recent (i.e., post-CI) activity of the Campi Flegrei volcano.

5.2. Tephra correlations

To correlate the investigated units of the Campanian Plain with MIS 5 Mediterranean tephra markers, we refer to the Central Mediterranean tephrostratigraphic successions spanning this interval that (i) record in stratigraphic order most MIS 5 tephra markers, (ii) have a good geochemical characterization of all tephra, (iii) have a good radioisotopic or stratigraphic chronology, and (iv) have a good expression of the MIS 5 climate variability, which enable a reliable assessment of the tephra climato-stratigraphic position.

These requisites are fully or partially met by (i) the rich tephrostratigraphic record of the Lago Grande di Monticchio, southern Italy (Fig. 1a), located ca. 120 km east of the Neapolitan volcanoes – thus in an ideal position for recording their explosive activity (Wulf et al., 2004, 2012) – and (ii) the Popoli MIS 5 succession, in Sulmona Basin (Fig. 1a), where MIS 5 tephra were dated by $^{40}Ar/^{39}Ar$ method (Giaccio et al., 2012; Regattieri et al., 2017), allowing a direct, unambiguous comparison with the $^{40}Ar/^{39}Ar$ chronology here obtained for the investigated Campanian Plain units.

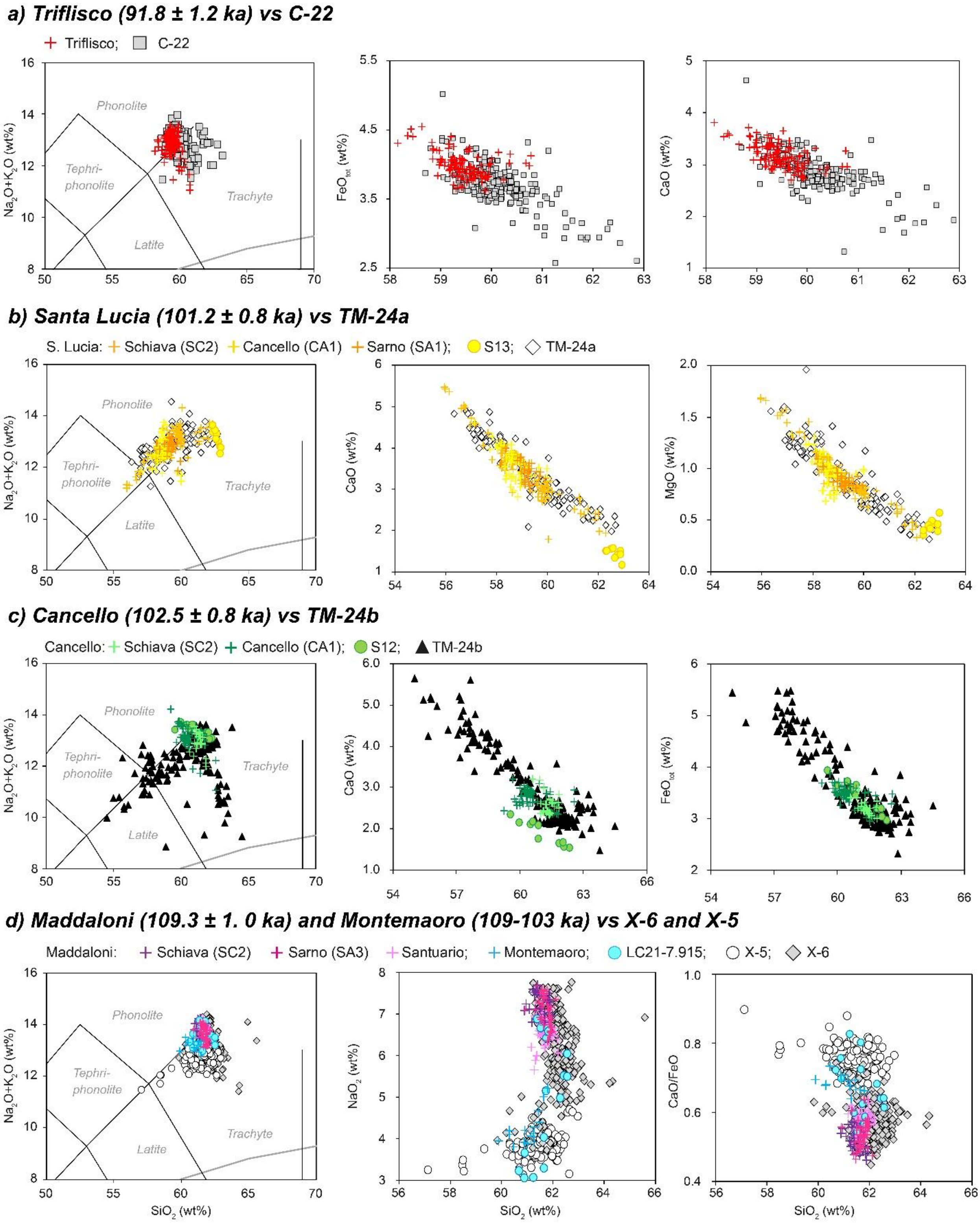

Figure. 5. Major element bi-plots and ratios of Triflisco, Santa Lucia, Cancello, Montemaoro and Maddaloni units from the Campanian Plain in comparison with literature data. Literature EDS data source: SC2-b (Di Vito et al., 2008), S13, S12 (Munno and Petrosino, 2007). Literature glass-WDS data source: C-22 marker = TM-23-11 (Wulf et al., 2004), POP-1 (Giaccio et al., 2012), PRAD-2525 (Bourne et al., 2015), TF-10 (Giaccio et al., 2017a), TP05-25.195 (Wulf et al., 2018); TM-24a marker = TM-24a (Wulf et al., 2012), POP-2 (Regattieri et al., 2015); TM-24b marker = TM-24b (Wulf et al., 2012), POP-2A (Giaccio et al., 2012), OH-DP-0404 (Leicher et al., 2016), TF-11 (Giaccio et al., 2017a); X-5 marker = TM-25 (Wulf et al., 2012), POP-3, CIL-1 (Giaccio et al., 2012), LeS1 (Donato et al., 2016), TF-12 (Giaccio et al., 2017a), LC21-7.915 (Satow et al., 2015); X-6 marker = TM-27 (Wulf et al., 2012, 2018), CIL-2 (Giaccio et al., 2012), I-9 (Insinga et al., 2014), POP-4 (Regattieri et al., 2015), PRAD-2812 (Bourne et al., 2015), OH-DP-0435 (Leicher et al., 2016), Tarsia, LeS2 (Donato et al., 2016),TF-13 (Giaccio et al., 2017a), TP05-27.915 (Wulf et al., 2018), Cavallo-G (Zanchetta et al., 2018).

Triflisco - Both $^{40}Ar/^{39}Ar$ chronology and major elements (Fig. 5a) glass composition of Triflisco unit (91.8 ± 1.4 ka) are fully consistent with those of the Sulmona tephra POP1 (92.1 ± 4.6 ka; Giaccio et al., 2012) that, in turn, was correlated to the Monticchio tephra TM-23-11 (Giaccio et al., 2012; Fig. 5a), dated at 95.18 ± 4.76 ka (Wulf et al., 2012). POP1/TM-23-11 was also correlated to the widespread C-22 tephra marker (Giaccio et al., 2012) of the Tyrrhenian Sea tephra series (Paterne et al., 1986, 1988). The correlation of Triflisco with POP1//TM-23-11/C-22 is supported also by incompatible trace element contents plotted against Th (Fig. 6a). Furthermore, $^{87}Sr/^{86}Sr$ isotope ratios of Triflisco perfectly match literature values for the POP1/TM-23-11/C-22 tephra layers/markers (Fig. 3a), strengthening this correlation.

The POP1/TM-23-11/C-22 was also identified in Fucino succession, as layer TF-10 (Giaccio et al., 2017a), and in San Gregorio Magno basin, as layer S14, (Munno and Petrosino, 2007; Petrosino et al. 2019; Fig. 1a). The C-22 was also correlated to the 11 cm- thick tephra layer CET1-10/14 in the Tyrrhenian core CET-1 (Petrosino et al., 2016). This marker was also identified in the marine core PRAD 1-2, in the Adriatic Sea, as layer PRAD-2517 (Giaccio et al., 2012; Bourne et al., 2015). Finally, in the peatland succession of Tenaghi Philippon, in Greece (Figs. 1a, 7), recent cryptotephra investigations by Wulf et al. (2018) allowed the correlation of the C-22 marker with tephra layer TP05-25.195 (Fig. 5a).

Santa Lucia – Both major (Fig. 5b) and trace (Fig. 6a) element compositions, as well as the chronology of Santa Lucia unit are compatible with TM-24a tephra of Monticchio, to which the Sulmona tephra POP2 was also correlated (Giaccio et al., 2012; Fig. 7). The Monticchio varve-supported age for TM-24a is 102.0 ± 5.7 ka (Wulf et al, 2012; Monticchio chronology MON-2014, Sabine Wulf, personal communication 2017), whereas the modelled age of POP2 is 102.0 ± 2.4 ka (Regattieri et al., 2015). In Sulmona paleo-hydrological record, POP2 falls in the early stage of a period of increasing precipitation correlated to the Greenland Interstadial 23, which in reference records (e.g., Corchia Cave, North Greenland Ice Core Project members et al., 2004; Drysdale et al., 2007) starts about 102-103 ka, thus in agreement with the estimated age of POP2/TM-24a. Here Santa Lucia unit is precisely $^{40}Ar/^{39}Ar$ dated at 101.2 ± 0.8 ka (Fig. 4b), supporting this correlation. $^{87}Sr/^{86}Sr$ isotope ratios determined on Santa Lucia samples show values similar to those obtained for Triflisco/C-22 tephra layer/marker (Fig. 3a), but they can be discriminated based on the higher HFSE (e.g., Th, U) contents of the Triflisco/C-22 glasses than the Santa Lucia ones, thus preventing erroneous correlations (Fig. 6a).

At Fucino Basin (Figs. 1a, 7), tephra layer TF-11, located immediately below tephra layer TF-10/C-22, was correlated by Giaccio et al. (2017a) to the Monticchio tephra POP2/TM-24a (Fig. 7). The same marker horizon was also recognized in Lake Ohrid (North Macedonia-Albania; Figs, 1a, 7) as layer OH-DP-0404 (Leicher et al., 2016). The crypto-tephra CET1 12-13-14 in the Tyrrhenian core CET1 (Fig. 1a) also has major element composition compatible with TM-24a/POP2 (Petrosino et al., 2016), thus representing the unique so far known occurrence of Santa Lucia unit in the marine realm. Finally, at San Gregorio Magno (Munno and Petrosino, 2007; Petrosino et al., 2019), tephra layer S13, underlying tephra layer S14/C-22, would be stratigraphically well suited to be a potential candidate for the TM-24a/Santa Lucia unit (Fig. 7). However, EDS-glass chemical composition supports only partially this correlation (Fig. 5b), and WDS-glass composition should be acquired on purpose.

***Cancello* –** The Cancello pumice fall occurs below Santa Lucia unit=TM-24a/POP2 (Di Vito et al., 2008; Fig. 1b), thus indicating POP2a (Giaccio et al., 2012) and TM-24b (Wulf et al., 2012), which respectively underlay POP2 and TM-24a, as the best candidates for correlation to this unit (Fig. 7). Major element biplots confirm this correlation (Fig. 5c), also supported by trace element comparison (Fig. 6a). In particular, with respect to the Santa Lucia unit, the Cancello unit appears to extend to lower Th contents (Figs. 2f, 6a), which allows discriminating these two tephra markers. At Monticchio, TM-24b is varve-dated at 103.1 ± 5.7 ka (Wulf et al., 2012; MON-2014), while in Sulmona Basin a modelled age of 103.3 ± 1.4 ka was obtained for POP2a (Regattieri et al., 2015), in agreement with the more precise age of 102.5 ± 0.8 ka here measured for the Cancello unit (Fig. 4c). In summary, the correlation of Cancello unit to POP2a/TM-24b is fully supported by all the geochemical and geochronological data.

At San Gregorio Magno (Munno and Petrosino, 2007; Petrosino et al., 2019), the tephra layer S12 is stratigraphically well suited for being a good correlation candidate for POP2a/TM-24b (Fig. 7). The geochemical correlation of S12 with Cancello unit, based on the available EDS-glass composition, is quite convincing (Fig. 5c), but more compelling WDS data would be required. Finally, the crypto-tephra CET1-15 in the Tyrrhenian core CET1 (Fig. 1a) is stratigraphically (Fig. 7) and compositionally consistent with TM-24b/POP2b (Petrosino et al., 2016).

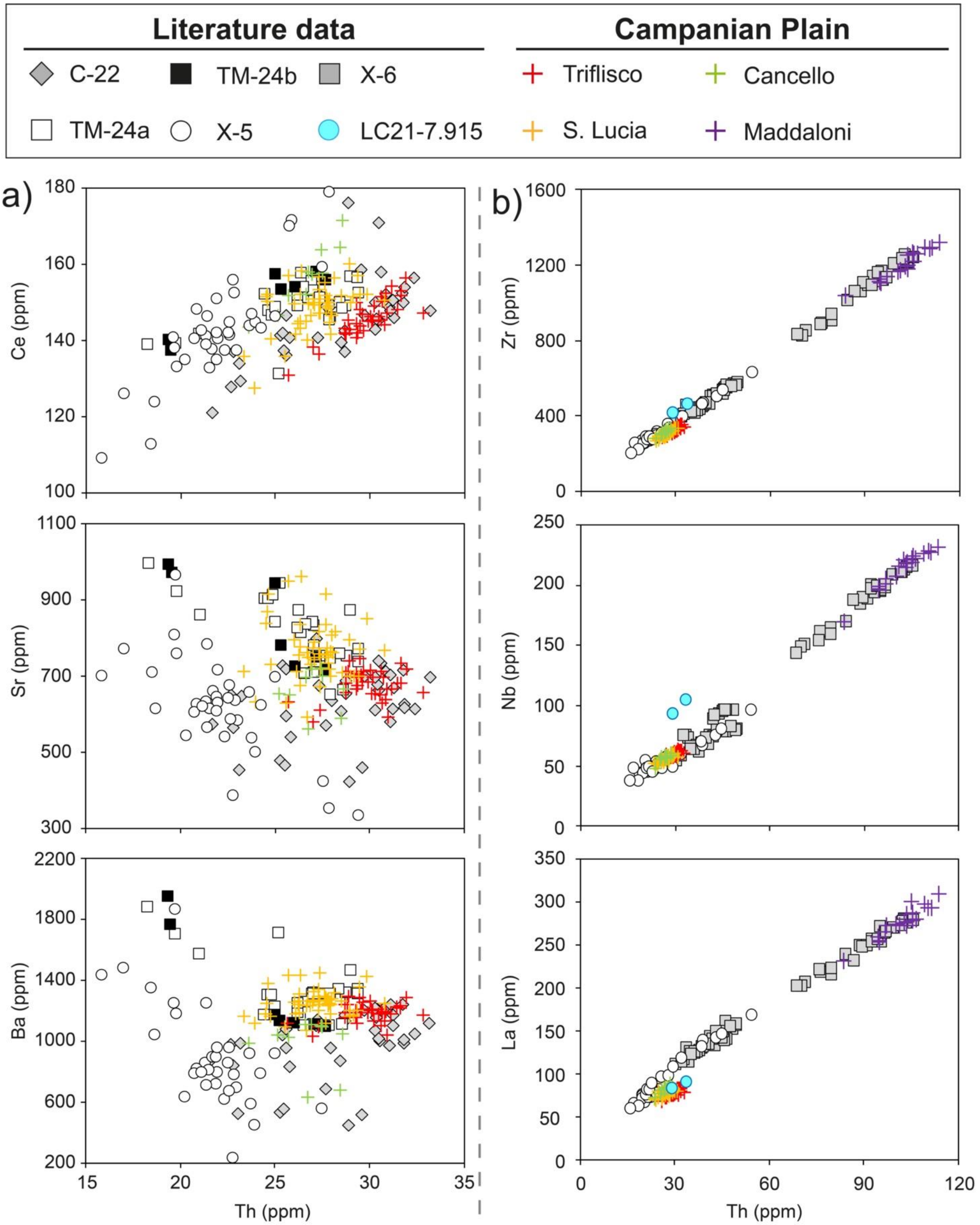

Figure. 6. Incompatible trace element patterns against Th for the Triflisco, Santa Lucia, Cancello and Maddaloni units in comparison with literature data. Literature data source: C-22 = TM-23-11, PRAD 2525 (Bourne et al., 2015), S14 (Petrosino et al., 2019); TM-24a = TM-24a (Wulf et al., 2012); TM-24b = TM-24b (Wulf et al., 2012); X-5 = TM-25 (Wulf et al., 2012), POP-3 (Giaccio et al., 2012), LC21-7.915 (Satow et al., 2015), LeS1 (Donato et al., 2016), TF-12 (Giaccio et al., 2017a), S11 (Petrosino et al., 2019); X-6 = TM-27, PRAD 2812 (Bourne et al., 2015), LeS2 (Donato et al., 2016), TF-13 (Giaccio et al., 2017a), S10 (Petrosino et al., 2019).

Maddaloni and Montemaoro – At Masseria Montemaoro quarry (Fig. 1a), these two, stratigraphically superimposed units underlie the Cancello unit (Fig. 1c). The $^{40}Ar/^{39}Ar$ age of 109.3 ± 1.0 ka determined for

Maddaloni unit is virtually indistinguishable from that of 109.1 ± 0.8 ka, obtained for the Sulmona tephra layer POP4 (Regattieri et al., 2017), which was correlated to the X-6 tephra marker (Regattieri et al., 2015), corresponding to the Monticchio TM-27 (Wulf et al., 2012). Consistent with this chronological information, the major (Fig. 5d) and trace (Fig. 6b) elements composition of the Maddaloni unit well match the most evolved term of POP4/TM-27 tephra layer/marker and those of the other X-6 equivalent layers in distal archives through the central Mediterranean area (Fig. 1a). Sr-Nd isotope values obtained from the Maddaloni unit are consistent with those of CIL-2/X-6 tephra layer/marker from the Cilento coast and other X-6 occurrences (Fig. 3a-b), thus further supporting its correlation with the X-6 marker. Moreover, major and trace elements glass compositions are extremely distinctive (e.g., different alkali ratio and Cl content, incompatible trace element patterns), and we thus highly recommend the employment of these geochemical tracers as a correlation tool for the X-6 tephra (Figs. 5d, 6b; Supplementary Materials-1). All geochemical and chronological data thus corroborate Maddaloni as the most proximal equivalent of the X-6 tephra marker.

The Ionian X-6 tephra marker (Keller et al., 1978), and its other marine and terrestrial equivalents, is the most widespread MIS 5 Campi Flegrei tephra (Figs. 1a, 7), while considering the whole Campi Flegrei record, in terms of dispersal area it is second only to the CI (e.g., Costa et al., 2012). It has been recognised in a series of sedimentary successions in the central Mediterranean area (Figs. 1a, 7), including the Ionian Sea (I-9, Insinga et al., 2014), Tyrhhenian Sea (C-31, Paterne et al., 2008), Adriatic Sea (PRAD-2812, Bourne et al. 2015), Fucino Basin (TF-13, Giaccio et al., 2017a), Cilento Coast (Giaccio et al., 2012; Donato et al., 2016), San Gregorio Magno Basin (S10, Petrosino et al., 2019), Valle del Crati (Tarsia, Donato et al., 2016), Grotta del Cavallo Palaeolithic site (Unit G, Zanchetta et al., 2018), Lake Ohrid (OH-DP-0435, Leicher et al., 2016), and Tenaghi Philippon (TP05-27.915, Wulf et al., 2018).

Regarding Montemaoro unit, its stratigraphic position between Maddaloni/X-6 and Cancello/TM-24b, which chronologically constrains it between ~109 ka and ~103 ka, makes it the best candidate for the terrestrial counterpart of the Ionian Sea marker X-5, which lays immediately above the X-6 (Keller et al., 1978). The X-5 is equivalent to tephra layer TM-25 in the Lago Grande di Monticchio succession, dated at 105.6 ± 0.5 ka (recalculated with ACs at 1.1891 Ma; Tyrrhenian Sea; Petrosino et al., 2015), or POP3 $^{40}Ar/^{39}Ar$ dated at 105.8 ± 1.3 ka (Sulmona Basin, Giaccio et al., 2012). Although it was not possible to acquire new major (glass-WDS) and/or trace element data, the available glass-EDS composition for the Montemaoro unit supports this correlation (Fig. 5d). Consequently, we suggest that the Montemaoro unit is the most likely proximal counterpart of the X-5, based on the chronological and stratigraphical constraints provided in this study and the existing chemical data. Future discovery of a new field exposure of Montemaoro would allow further verification of this correlation.

Although less dispersed, the X-5 marker, like the X-6, was reported in several stratigraphic successions (Figs. 1a, 7), including the Fucino Basin (TF-12, Giaccio et al., 2017a), Cilento Coast (CIL1, Giaccio et al., 2012; LeS1, Donato et al., 2016), San Gregorio Magno Basin (S11, Petrosino et al., 2019), and as the lowermost tephra layer in CET1 core (i.e., CET1-18, Petrosino et al., 2015), $^{40}Ar/^{39}Ar$ dated at 105.18 ± 0.5 ka (2σ analytical uncertainty).

A potential correlative for either the X-6 or X-5 marker was also recognised at the remote site of marine core LC21 (Satow et al., 2015), in the Aegean Sea (Fig. 1a). Specifically, the crypto-tephra LC21-7.915, whose base was dated at 104.1 ± 2.2 ka, according to the LC21 age model (Satow et al., 2015), presents two geochemical compositions indicating both Santorini and Campanian sources. The Campanian component is in turn represented by two glass HAR and LAR trachyte-phonolite populations, which are compatible with X-5 and X-6 compositions, respectively (Fig. 5d). Moreover, in terms of trace element composition, the few available data appear quite consistent with both markers (Fig. 6b). However, both the age and climatostratigraphic position of the crypto-tephra LC21-7.915 make the X-5 the most probable correlative. Indeed, LC21-7.915 precisely marks the onset of the sapropel S4 deposition, at the base of which in the Tyrrhenian Sea records the tephra X-5/C-27 is also found (Fig. 8; Paterne et al., 2008; Regattieri et al., 2015). Therefore, we are inclined to consider the X-5 as the most likely correlative for the HAR component of the Campanian portion of LC21-7.915 crypto-tephra, though the co-presence of the LAR component would require a plausible explanation.

Overall, the correlations of the investigated Campanian Plain units with the five distal tephra markers are well supported by several line of consistent, independent evidence, including their stratigraphic order, geochronology, and geochemistry (major and trace elements, and the Sr-Nd isotopes). However, in some cases, the geochemical variability of the investigated Campanian Plain units is less wide than the corresponding distal tephra. This is especially true for Cancello and Maddalloni units, the composition of which covers only a part of the wider variability observed in distal settings (Figs. 5c-d and 6b). This is not surprising, as the occurrence of the analysed medial units is relatively scant with respect to the distal ones, and thus could be not representative of the complete eruptive sequence and geochemical variability. This would suggest that not all the eruptive phases or sub-units, e.g., pyroclastic flow or fall, of Cancello and Maddaloni units reached the distance of 30-40 km, at which the investigated sections are located (Fig. 1b) or had dispersal axes not compatible with pumice deposition in these localities.

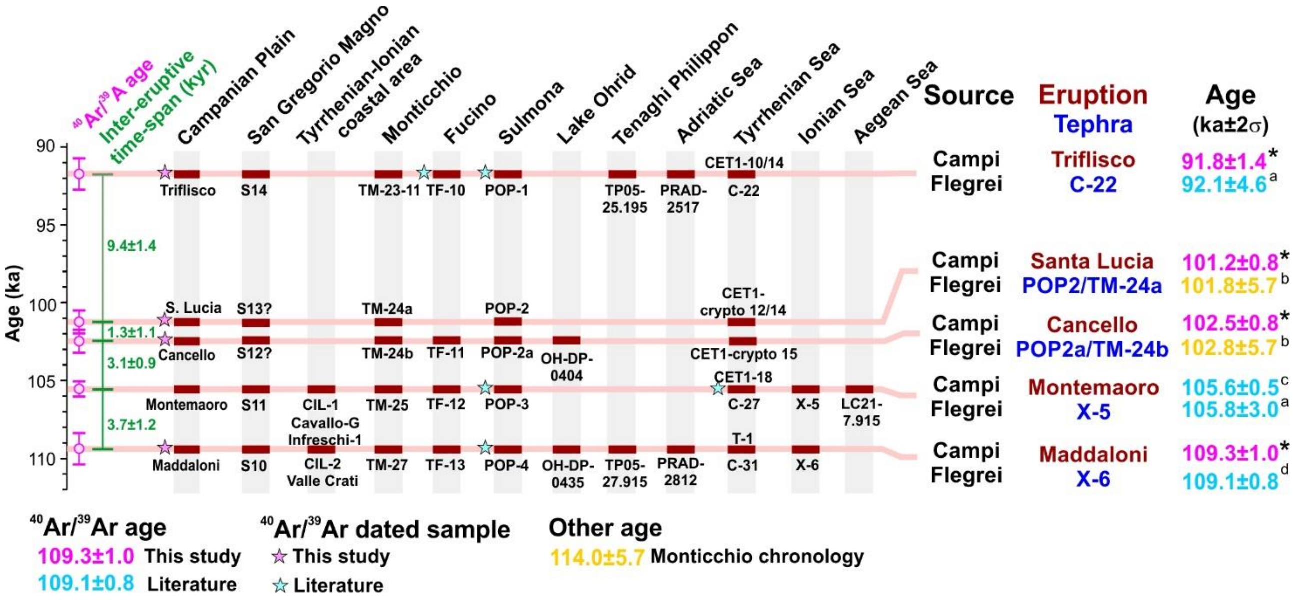

Figure 7. Age and occurrences of the C-22, POP2/TM-24a, POP2a/TM-24b, X-5, and X-6 tephra markers in terrestrial and marine sedimentary environments through the Mediterranean region. ^{40}Ar/^{39}Ar ages are according to ACs at 1.1891 Ma and FCs at 28.294 Ma. * This study, [a] Giaccio et al. (2012); [b] Wulf et al. (2012); [c] Petrosino et al. (2016); [d] Regattieri et al. (2015).

5.3. Implications for the chronology of the millennial-scale climatic oscillations of the MIS 5c-d

The great relevance of some of the investigated tephra layers as fundamental chronological and stratigraphic markers for the Mediterranean MIS 5c-d high frequency climatic variability was widely acknowledged and discussed in previous papers (e.g., Giaccio et al., 2012; Regattieri et al., 2015). However, the acquisition of new high-precision ^{40}Ar/^{39}Ar ages for two previously undated tephra (Cancello/TM-24b and Santa Lucia/TM-24a tephra layers/markers), the substantial improvement in accuracy of the Triflisco/C-22 unit, as well as the acquisition of new high-resolution records containing these tephra markers (e.g., Tenaghi Philippon; Wulf et al., 2018), give us the opportunity to discuss the implications of these new data from a palaeoclimatological perspective, in particular on the timing and spatial synchronicity of MIS 5c-d climatic variability.

For this purpose, we consider the records endowed with suitable resolution and good expression of the millennial scale climate oscillations of the MIS 5d-c, which can be reasonably correlated to the succession of stadial and interstadial events documented in the reference record of the Greenland ice (e.g., North Greenland Ice Core Project members et al., 2004). These are (i) the Lago Grande di Monticchio pollen profile, Southern Italy (e.g., Brauer et al., 2007; Wulf et al., 2012), (ii) the isotope series of Sulmona Basin, Central Italy (Regattieri et al., 2015, 2017), (iii) the Tenaghi Philippon pollen record, in Greece (Milner et al., 2012, 2013, 2016), and (iv) the pollen record of Lake Ohrid, North Macedonia-Albania (Sinopoli et al., 2018; Figs. 1a, 8). For the sapropel stratigraphy, we also consider the Tyrrhenian Sea record of the core KET 8004 (Paterne et al, 2008), which contains three out of the five markers (Fig. 8), and the Aegean Sea core LC21, likely containing the X-5 layer (Satow er al., 2015; Fig. 8).

So far, Monticchio and Sulmona are the only Mediterranean records containing all the five MIS 5d-c tephra from Campi Flegrei (Fig. 8), whereas Tenaghi Philippon and Ohrid contain only two markers, i.e., Maddaloni/X-6 and Triflisco/C-22, and Maddaloni/X-6 and Santa Lucia/TM-24a, respectively (Fig. 8; Table 2).

The Maddaloni/X-6 unit, the most common tephra in the considered records (Fig. 7), occurs at the very end of a short interstadial pulsation, likely corresponding to Greenland Interstadial (GI) 25_a. It precedes the onset of the first marked stadial oscillation of the MIS 5 period, the Greenland Stadial (GS) 25_a, corresponding to the North Atlantic cold event C24 (e.g., Shackleton et al., 2004; Fig. 8). The temporal offset, i.e., the difference between the radioisotopic $^{40}Ar/^{39}Ar$ age of Maddaloni/X-6 tephra and the age reported in the various paleoclimatic records (Δt in Fig. 8), is small, reaching the maximum value of ca. 1 kyr in the Monticchio record (Fig. 8; Table 2). However, assuming that the inferred position of Maddaloni/X-6 tephra layer/marker in the Greenland isotope record is correct, then, the age of the end of the GI-25_a, 110.6 ka, according to GICC05 (Rasmussen et al., 2014), should be approximately 1.3 kyr younger (Fig. 8). On the contrary, Sardinian stalagmite evidence suggests instead that the GI-25_b ended at 110.5 ka (Columbu et al., 2017), which is fully consistent with the GICC05 chronology.

The Montemaoro/X-5 tephra occurs in the medial of an interstadial oscillation correlated to the GI-24 (e.g., Regattieri et al., 2015). More precisely, Montemaoro/X-5 tephra occurs close to a very brief stadial pulsation within the GI-24 that is quite evident in all the considered records and that likely corresponds to the short GS-24.2 (Fig. 8). The Δt, relative to the Montemaoro/X-5 tephra, is of ca. 1 kyr in all records, except Monticchio, in which it is negligible (Fig. 8; Table 2). In the Tyrrhenian Sea, and likely in the Aegean Sea, the Montemaoro/X-5 also represents an excellent marker for the Sapropel S4, which is in turn correlated to the GI-24.1 (Regattieri et al., 2015; Fig. 8).

The Cancello and Santa Lucia tephra layers form an interesting couplet of temporally closely related tephra, which mark the onset of an interstadial and the ensuing stadial phase, likely corresponding to the GI-23.2 and the GS-23.2, respectively (Fig. 8). In all the considered records, the negligible Δt relative to this couple of tephra evidences a good agreement between the $^{40}Ar/^{39}Ar$ chronology and the age models of the records (Fig. 8).

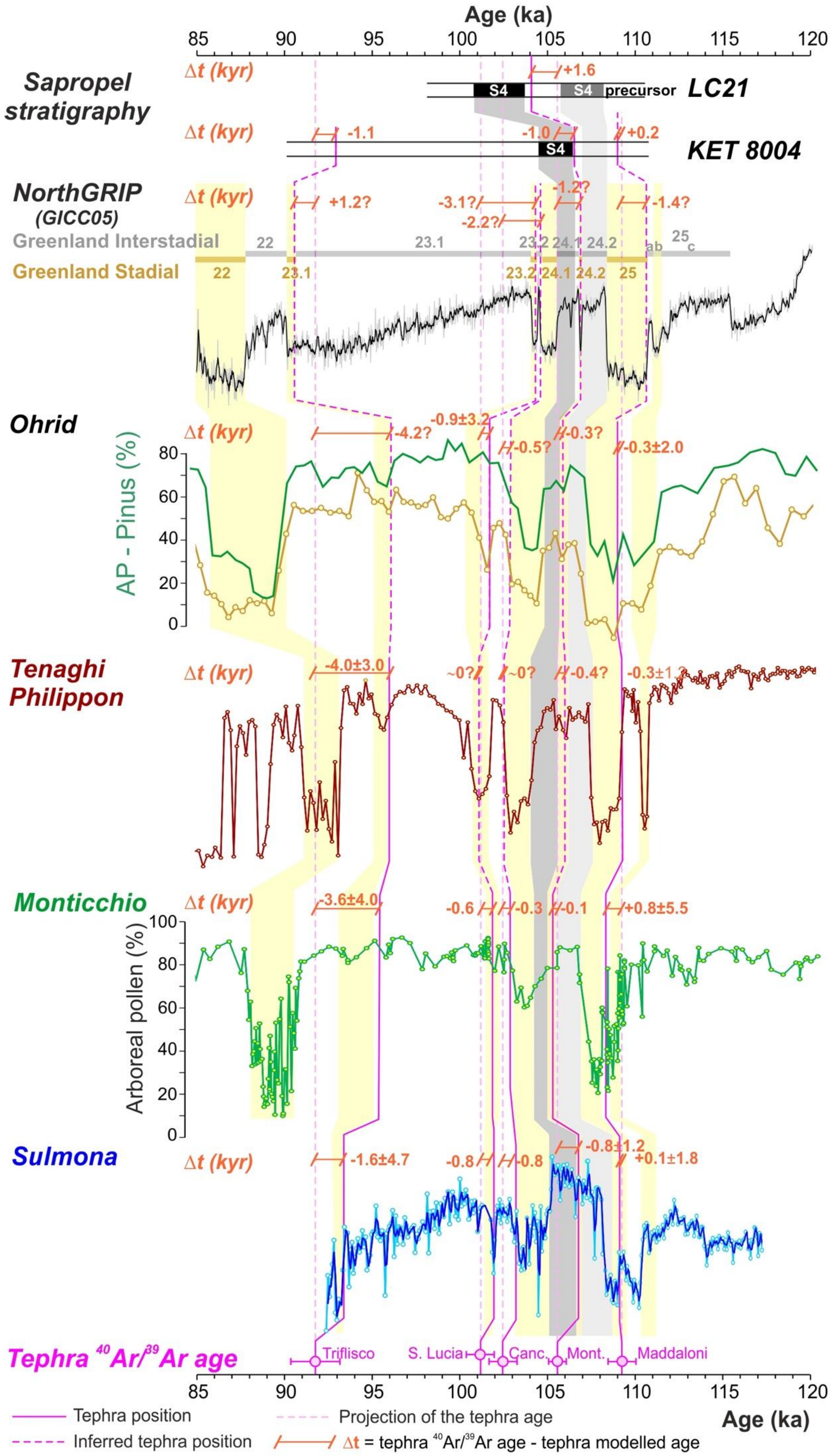

Age (ka)
Sapropel stratigraphy
Δt (kyr)
LC21
S4
S4 precursor
KET 8004
NorthGRIP (GICC05)
Greenland Interstadial
Greenland Stadial
δ18O (‰)
Ohrid
AP - Pinus (%)
TOC (%)
Tenaghi Philippon
Arboreal pollen (%)
Monticchio
Sulmona
Tephra 40Ar/39Ar age
Triflisco
S. Lucia
Canc.
Mont.
Maddaloni
Tephra position
Inferred tephra position
Projection of the tephra age
Δt = tephra 40Ar/39Ar age - tephra modelled age

654

Figure 8. Chronological offset between ^{40}Ar/^{39}Ar and modelled tephra age in selected high-resolution Mediterranean records containing the here investigated tephra and showing the millennial-scale climatic oscillations of the MIS 5d-c, compared to Greenland ice succession of stadial-interstadial events (Rasmussen et al., 2014). The Mediterranean sapropel stratigraphy from the Tyrrhenian Sea core KET 8004 (Paterne et al., 2008) and Aegean Sea core LC21 (Satow et al., 2015), is also shown. The sapropel nomenclature is according to Ziegler et al. (2010). Data source: Lake Ohrid Arboreal pollen minus *Pinus* (AP – Pinus) and total organic carbon (TOC): Sinopoli et al. (2018), Wagner et al., (2017, 2019); Tenaghi Philippon pollen record: Milner et al. (2012, 2013, 2016); Monticchio pollen record; Brauer et al. (2007); Sulmona isotope record, Regattieri et al (2015).

Finally, the Triflisco/C-22 tephra occurs at the beginning of a stadial event that interrupts a relatively long interstadial period, likely corresponding to the GS-23.1, which occurs at the end of the long-term cooling period featuring the GI-23.1 (Fig. 8). Noteworthy, the Δt relative to this tephra is quite long for the Monticchio and Tenaghi Philippon pollen records, reaching the considerable value of ca. 4 kyr (Fig. 8). The Δt is instead quite negligible for the NorthGRIP record (~1.2 kyr), provided that the inferred climatostratigraphic position of Triflisco/C-22 in the Greenland record is correct.

In summary, the Δt is relatively little for most of the climatic events, for which the Campi Flegrei MIS 5 tephra act as fundamental markers, and generally do not exceed the uncertainty associated to both ^{40}Ar/^{39}Ar ages and the age models of the respective paleoclimatic records (Table 2). However, the event associated with the Triflisco/C-22 represents a notable exception, for which the Δt can exceed the uncertainty associated to the ^{40}Ar/^{39}Ar dating of Triflisco/C-22 and of the paleoclimatic record age models (Figs. 7, 8; Table 2). With this regard, we emphasize that such wide Δt cannot be explained invoking an uncertainty of the tephra position within the records, as, at least for Monticchio and Tenaghi Philippon), where the Δt is -3.6 ± 4.0 kyr and -4.0 ± 3.0 kyr (Table 2), it is not relayed on an inference, this being based on undisputable stratigraphic evidence (Fig. 8).

Overall, the investigated tephra can be considered good stratigraphic markers of some of the stadial-interstadial events, as well as of the very short sub-stadial and sub-interstadial oscillations that punctuated the MIS 5c-d climatic variability (Table 2), whose chronology can greatly benefit from the high precision ^{40}Ar/^{39}Ar dating of the Campi Flegrei eruption products.

Table 2. Detailed climatostratigraphic position of the Campi Flegrei units with respect to the millennial to sub-millennial scale MIS 5 paleoclimatic events as recorded in reference archives of the central Mediterranean area (Figs. 1, 7 and 8). The temporal offset, i.e., the difference between the radioisotopic ^{40}Ar/^{39}Ar age of Campi Flegrei tephra and the age of the corresponding distal tephra, as reported in the various paleoclimatic records, is also shown. Data source: Sulmona: Regattieri et al. (2015, 2017); Monticchio: Wulf et al. (2012), Regattieri et al. (2015); Ohrid: Leicher et al. (2021); Tenaghi-Philippon: Wulf et al. (2018); LC21: Satow et al. (2015).

Campanian Plain	**Sulmona**	**Monticchio**	**Ohrid**	**Tenaghi-Philippon**	**LC21**	
Tephra ^{40}Ar/^{39}Ar age (ka±2σ)	Tephra Age±2σ ka Δt±2σ kyr	Tephra Age±2σ ka Δt±2σ kyr	Tephra Age±2σ ka Δt±2σ kyr	Tephra Age±2σ ka Δt±2σ kyr	Tephra Age±2σ ka Δt±2σ kyr	**Correlated event**
Triflisco 91.8±1.4	POP1 93.4±4.5	TM-23-11 95.4±3.8		TP05-25.195		Onset of the GS-23.1

	-1.6±4.7	-3.6±4.0		95.8±2.6 -4.0±3.0		
Santa Lucia 101.2±0.8	POP2 102.0±2.4 -0.8±2.5	TM-24a 101.8±5.0 -0.6±5.1	OH-DP-0404 102.1±3.1 -0.9±3.2			Middle part of the GS-23.2
Cancello 102.5±0.8	POP2a 103.3±1.4 -0.8±1.6	TM-24b 102.8±5.1 -0.3±5.2				Onset of the GI-23.2
Montemaoro 105.6±0.5	POP3 106.4±1.1 -0.8±1.2	TM-25 105.5±5.3 0.1±5.3			LC21-7.915 104.0±2.0 1.6±.1	End of the GS-24.2 - base of the sapropel S4
Maddaloni 109.1±0.8	POP4 109.0±1.5 0.1±1.8	TM-27 108.3±5.4 0.8±5.5	OH-DP-0435 109.4±1.8 -0.3±2.0	TP05-27.915 109.4±0.9 -0.3±1.2		Onset of the GS-25 - End GI-25a

6. Conclusions

In this study, we presented a wide dataset (i.e., stratigraphy, major, minor, and trace elements, Sr-Nd isotopic composition and $^{40}Ar/^{39}Ar$ ages) required for a full characterization of four pumice fall deposits, named Triflisco, Santa Lucia, Cancello, and Maddaloni, occurring in the Campanian Plain, 30 to 60 km east of the Campi Flegrei volcanic field, and stratigraphically laying below the CI (~40 ka). Based on these data, these units are here attributed to a previously unknown 109-92 ka explosive activity at Campi Flegrei volcano and correlated with the widespread C-22, TM-24a/POP-2, TM-24b/POP-2a and X-6 tephra markers, respectively. Furthermore, the chronological and stratigraphic constraints provided in this study, and a review of previous EDS data, allow us also to propose the correlation of a fifth unit (i.e., Montemaoro) with the X-5 marine tephra marker as well.

Our data confidently allow us to trace the volcanic source of these fundamental Mediterranean marker horizons, so far only hypothesized. This extends the activity history of the Campi Flegrei volcano back ~110 ka at least, setting the groundwork for a reassessment of the volcanic history, and related hazards, and confirming the Campi Flegrei volcano as one of the Europe's most productive sources of widespread and disruptive ash fall events. The Maddaloni/X-6, given its wide dispersal area, clearly arises from one of the largest explosive events through the whole Campi Flegrei eruptive history and demands further volcanological investigations.

The new high-precision $^{40}Ar/^{39}Ar$ dating of the investigated units provide new fundamental temporal constraints for refining and consolidating the chronology of MIS 5d-c period, characterised by a marked millennial- to sub-millennial scale climatic variability, well documented in Mediterranean archives. Specifically, the ages obtained for the Cancello and Santa Lucia tephra markers provide two new chronological constraints for the climatic oscillations likely corresponding to the Greenland interstadial GI-23.2 and Greenland stadial GS-23.2. Furthermore, the improved precision of the age for Triflisco would imply a substantial extension of the duration of the interstadial period corresponding to the GI-23.1 up to 92 ka, i.e., ~4 kyr later than the ~96 ka age reported for the GI-23.1 in several reference Mediterranean records. (Fig. 8). A reappraisal of the related chronologies is thus required.

Future research development on the eruptive history and long-term hazard assessment at Campi Flegrei, as well as paleoclimatic and archaeological investigations in central Mediterranean, will greatly benefit from the geochemical and geochronological dataset provided in this contribution. Given the strong geochemical similarities of the HAR Triflisco/C-22, Santa Lucia/TM-24a, and Cancello/TM-24b units, we encourage caution to avoid potentially misleading correlations based solely on major elements. Therefore, especially when a specific tephra layer occurrence lacks bracketing tephra units, we recommend integrating major element data with trace element and Sr-Nd isotope analysis, as they proved to be the best discriminating tool for these tephra deposits.

Acknowledgments

R. Jedlička and M. Racek, E. Braschi and A. Orlando, are thanked for providing valuable technical assistance during EPMA analysis at Prague and Florence Universities respectively. Field activities were financially supported by "Sapienza" University, "Bando di Avvio alla Ricerca", protocol N° AR120172AD35B81D (responsible: L.M.). The INGV-OV laboratories have been also financially supported by the EPOS Research Infrastructure through the contribution of the Italian Ministry of University and Research (MUR). P.G.A. is funded through a UK Research and Innovation Future Leaders Fellowship (MR/S035478/1).

References

Albert, P.G., Giaccio, B., Isaia, R., Costa, A., Niespolo, E.M., Nomade, S., Pereira, A., Renne, P.R., Hinchliffe, A., Mark, D.F., Brown, R.J., Smith, V.C., 2019. Evidence for a large-magnitude eruption from Campi Flegrei Caldera (Italy) at 29 ka. *Geology.* **47** (7), 595-599. https://doi.org/10.1130/G45805.1.

Albert, P.G., Hardiman, M., Keller, J., Tomlinson, E.L., Smith, V.C., Bourne, A.J., Wulf, S., Zanchetta, G., Sulpizio, R., Müller, U.C., Pross, J., Ottolini, L., Matthews, I.P., Blockley, S.P.E., Menzies, M.A., 2015. Revisiting the Y-3 stratigraphic marker: a new diagnostic glass geochemistry, age estimate, and details on its climatostratigraphical context. *Quat. Sci. Rev.* **118**, 105-121. https://doi.org/10.1016/j.quascirev.2014.04.002.

Andronico, D. & Cioni, R., 2002. Contrasting styles of Mount Vesuvius activity in the period between the Avellino and Pompeii Plinian eruptions, and some implications for assessment of future hazards. *Bull. Volcanol.* **64**, 372-391. https://doi.org/10.1007/s00445-002-0215-4.

Arienzo, I., Civetta, L., Heumann, A., Wörner, G., Orsi, G., 2009. Isotopic evidence for open system processes within the Campanian Ignimbrite (Campi Flegrei-Italy) magma chamber. *Bull. Volcanol.* **71**, 285-300. https://doi.org/10.1007/s00445-008-0223-0.

Arienzo, I., D'Antonio, M., Di Renzo, V., Tonarini, S., Minolfi, G., Orsi, G., Carandente, A., Belviso, P., Civetta, L., 2015. Isotopic microanalysis sheds light on the magmatic endmembers feeding volcanic eruptions: The Astroni 6 case study (Campi Flegrei, Italy). *J. Volcanol. Geotherm. Res.* **304**, 24–37. https://doi.org/10.1016/j.jvolgeores.2015.08.003.

Arienzo, I., Mazzeo, F.C., Moretti, R., Cavallo, A., D'Antonio, M., 2016. Open-system magma evolution and fluid transfer at Campi Flegrei caldera (Southern Italy) during the past 5 ka as revealed by geochemical and isotopic data: the archetype of Nisida eruption. Chem. Geol. **427**, 109-124. https://doi.org/10.1016/j.chemgeo.2016.02.007.

Arienzo, I., Moretti, R., Civetta, L., Orsi, G., Papale, P., 2010. The feeding system of the Agnano-Monte Spina eruption Campi Flegrei, Italy): dragging the past into present activity and future scenarios. *Chem. Geol.* **270** (1-4), 135-147. https://doi.org/10.1016/j.chemgeo.2009.11.012.

Balbas, A., Koppers, A.A.P., Kent, D.V., Konrad, K., Clark, P.U., 2016. Identification of the short-lived Santa Rosa geomagnetic excursion in lavas on Floreana Island (Galapagos) by $^{40}Ar/^{39}Ar$ geochronology. *Geology* **44** (5), 359-362 (2016). https://doi.org/10.1130/G37569.1.

Bourne, A.J., Albert, P.G., Matthews, I.P., Trincardi, F., Wulf, S., Asioli, A., Blockley, S.P.E., Keller, J., Lowe, J.J., 2015. Tephrochrunology of core PRAD 1-2 from the Adriatic Sea: insights into Italian explosive volcanism for the period 200-80 ka. *Quat. Sci. Rev.* **116**, 28-43. https://doi.org/10.1016/j.quascirev.2015.03.006.

Bourne, A.J., Lowe, J.J., Trincardi, F., Asioli, A., Blockley, S.P.E., Wulf, S., Matthews, I.P., Piva, A., Vigliotti, L., 2010. Distal tephra record for the last ca 105,000 years from core PRAD 1-2 in the central Adriatic Sea: implications for the marine tephrostratigraphy. *Quat. Sc. Rev.* **29**, 3079-3094. https://doi.org/10.1016/j.quascirev.2010.07.021.

Brauer, A., Allen, J.R.M., Mingram, J., Dulski, P., Wulf, S., Huntley, B., 2007. Evidence for the last interglacial chronology and environmental change from Southern Europe. *PNAS* **104** (2), 450-455. https://doi.org/10.1073/pnas.0603321104.

Brown, R.J., Civetta, L., Arienzo, I., D'Antonio, M., Moretti, R., Orsi, G., Tomlinson, E.L., Albert, P.G., Menzies, M.A., 2014. Geochemical and isotopic insights into the assembly, evolution and disruption of a magmatic plumbing system before and after cataclysmic caldera-collapse eruption at Ischia volcano (Italy). *Contirb. Mineral. Petrol.* **168**: 1035. https://doi.org/10.1007/s00410-014-1035-1.

Brown, R.J., Orsi, G., de Vita, S., 2008. New insights into Late Pleistocene explosive volcanic activity and caldera formation on Ischia. *Bull. Volcanol.* **70**, 583-603. https://doi.org/10.1007/s00445-007-0155-0.

Casalini, M., Heumann, A., Marchionni, S., Conticelli, S., Avanzinelli, R., Tommasini, S., 2018. Inverse modelling to unravel the radiogenic isotope signature of mantle sources from evolved magmas: the case-study of Ischia volcano. *Ital. J. Geosci.* **137**, pp. 00. https://doi.org/:103301/IJG.2018.05.

Civetta, L., Orsi, G., Pappalardo, L., Fisher, R.V., Heiken, G., Ort, M., 1997. Geochemical zoning, mingling, eruptive dynamics and depositional processes - the Campanian Ignimbrite, Campi Flegrei, Italy. *J. Volcanol. Geotherm. Res.* **75** (3-4), 183-219. https://doi.org/10.1016/S0377-0273(96)00027-3.

Columbu, A., Drysdale, R., Capron, E., Woodhead, J., De Waele, J., Sanna, L., Hellstrom, J., Bajo, P., 2017. Early last glacial intra-interstadial climate variability recorded in Sardinian speleothem. *Quat. Sci. Rev.* **169**, 391-397. https://doi.org/10.1016/j.quascirev.2017.05.007.

Costa, A., Folch, A., Macedonio, G., Giaccio, B., Isaia, R., Smith, V.R., 2012. Quantifying volcanic ash dispersal and impact of the Campanian Ignimbrite super-eruption. *Geophys. Res. Lett.* **39**, p. L101310. https://doi.org/10.1029/2012GL051605.

Cox, S.E., Hemming, S.R., Tootell, D., 2020 The Isotopx NGX and ATONA Faraday amplifiers. *Geochronology* **2**, 231-243. https://doi.org/10.5194/gchron-2-231-2020.

D'Antonio, M., Arienzo, I., Brown, R.J., Petrosino, P., Pelullo, C., Giaccio, B., 2021. Petrography and mineral chemistry of Monte Epomeo Green Tuff, Ischia Island, South Italy: Constraints for identification of the Y-7 tephrostratigraphic marker in distal sequences of the Central Mediterranean. *Minerals* **11**, 955. https://doi.org/10.3390/min11090955.

D'Antonio, M., Tonarini, S., Arienzo, I., CIvetta, L., Dallai, L., Moretti, R., Orsi, G., Andria, M., Trecalli, A., 2013. Mantle and crustal processes in the magmatism of the Campania region: inferences from mineralogy, geochemistry, and Sr-Nd-O isotopes of young hybrid volcanics of the Ischia island (South Italy). *Contrib. Mineral. Petrol.* **165**, 1173-1194. https://doi.org/10.1007/s00410-013-0853-x.

D'Antonio, M., Tonarini, S., Arienzo, I., Civetta, L., Di Renzo, V., 2007. Components and processes in the magma genesis of the Phlegrean Volcanic District, southern Italy. In: Beccaluva, L., Bianchini, G., Wilson, M. (eds.) Cenozoic Volcanism in the Mediterranean Area. *Geol. Soc. Am. Special Paper* **418**, 203-220.

De Astis, G., Pappalardo, L., Piochi, M., 2004. Procida volcanic history: new insights into the evolution of the Phlegrean Volcanic District (Campania region, Italy). *Bull. Volcanol.* **66**, 622-641. https://doi.org/10.1007/s00445-004-0345-y.

De Vivo, B., Rolandi, G., Gans, P.B., Calvert, A., Bohrson, W.A., Spera, F.J., Belkin, H.E., 2001. New constraints on the pyroclastic eruptive history of Campanian volcanic Plain (Italy). *Mineral. Petrol*. **73**, 47-65. https://doi.org/10.1007/s007100170010.

Deino, A.L., Orsi, G., de Vita, S., Piochi, M., 2004. The age of the Neapolitan Yellow Tuff caldera-forming eruption (Campi Flegrei Caldera - Italy) assessed by $^{40}Ar/^{39}Ar$ dating method. *J. Volcanol. Geotherm. Res.* **133** (1-4), 157-170. https://doi.org/10.1016/S0377-0273(03)00396-2.

Di Renzo, V., Arienzo, I., Civetta, L., D'Antonio, M., Tonarini, S., Di Vito, M.A., Orsi, G., 2011. The magmatic feeding system of the Campi Flegrei caldera: Architecture and temporal evolution. *Chem. Geol.* **281** (3-4), 227-241. https://doi.org/10.1016/j.chemgeo.2010.12.010.

Di Vito, M.A., Sulpizio, R., Zanchetta, G., D'Orazio M., 2008 The late Pleistocene pyroclastic deposits of the Campanian Plain: New insights into the explosive activity of the Neapolitan volcanoes. *J. Volcanol. Geotherm. Res.* **177**, 19-48. https://doi.org/10.1016/j.jvolgeores.2007.11.019.

Donato, P., Albert, P.G., Crocitti, M., De Rosa, C., Menzies, M.A., 2016. Tephra layers along the southern Tyrrhenian coast of Italy: Links to the X-5 & X-6 using volcanic glass geochemistry. J. *Volcanol. Geotherm. Res.* **317**, 30-41. https://doi.org/10.1016/j.jvolgeores.2016.02.023.

Drysdale, R., Zanchetta, G., Hellstrom, J.C., Fallick, A.E., McDonald, J., Catwright, I., 2007. Stalagmite evidence for the precise timing of North Atlantic cold events during the early last glacial. *Geology* **35** (1), 77-80. https://doi.org/10.1130/G23161A.1.

Fanara, S., Botcharnikov, R.E., Palladino, D.M., Adams, F., Buddensieck, J., Mulch, A., Behrens, H., 2015. Volatiles in magma related to Campanian Ignimbrite eruption: Experiments vs natural findings. *Am. Min.* **100** (10), 2284-2297. https://doi.org/10.2138/am-2015-5033.

Galli, P., Giaccio, B., Messina, P., Peronace, E., Amato, V., Naso, G., Nomade, S., Pereira, A., Piscitelli, S., Bellanova, J., Billi, A., Blamart, D., Galderisi, A., Giocoli, A., Stabile, T., Thil, F., 2017. Middle to Late Pleistocene activity of the Matese fault system (southern Apennines, Italy). *Tectonophysics* **699**, 61-81. https://doi.org/10.1016/j.tecto.2017.01.007.

Giaccio, B., Haydas, I., Isaia, R., Deino, A., Nomade, S., 2017b. High-precision ^{14}C and $^{40}Ar/^{39}Ar$ dating of Campanian Ignimbrite (Y-5) reconciles the time-scales of climatic cultural processes at 40 ka. *Sci. Rep.* **7**, 45940. https://doi.org/10.1038/srep45940.

Giaccio, B., Niespolo, E.M., Pereira, A., Nomade, S., Renne, P.R., Albert, P.G., Arienzo, I., Regattieri, E., Wagner, B., Zanchetta, G., Gaeta, M., Galli, P., Mannella, G., Peronace, E., Sottili, G., Florindo, F., Leicher, N., Marra, F., Tomlinson, E.L., 2017a. First integrated tephrochronological record for the last ~190 kyr from the Fucino Quaternary lacustrine succession, central Italy. *Quat. Sci. Rev.* **158**, 211-234. https://doi.org/10.1016/j.quascirev.2017.01.004.

Giaccio, B., Nomade, S., Wulf, S., Isaia, R., Sottili, G., Cavuoto, G., Galli, P., Messina, P., Sposato, A., Sulpizio, R., Zanchetta, G., 2012. The late MIS 5 Mediterranean tephra markers: a reappraisal from peninsular Italy terrestrial records. *Quat. Sci. Revi.* **56**, 31-45. https://doi.org/10.1016/j.quascirev.2012.09.009.

Goldstein, S.L., Denis, P., Oelkers, E.H., Rudnick, R.L., Walter, L.M., 2003. Standards for publication of isotope ratio and chemical data in chemical geology. *Chem. Geol.* **202**, 1-4. https://doi.org/10.1016/j.chemgeo.2003.08.003.

Insinga, D.D., Tamburrino, S., Lirer, F., Vezzoli, L., Barra, M., De Lange, G.J., Tiepolo, M., Vallefuoco, M., Mazzola, S., Sprovieri, M., 2014. Tephrochronology of the astronomically-tuned KC01B deep-sea core, Ionian Sea: insights into the explosive activity of the Central Mediterranean area during the last 200 ka. *Quat. Sci. Revi.* **85**, 63-84. https://doi.org/10.1016/j.quascirev.2013.11.019.

Iorio, M., Liddicoat, J., Budillon, F., Incoronato, A., Coe, R.S., Insinga, D.D., Cassata, W.S., Lubritto, C., Angelino, A., Tamburrino, S., 2014. Combined palaeomagnetic secular variation and petrophysical records to time-constrain geological and hazardous events: An example from the eastern Tyrrhenian Sea over the last 120 ka. *Glob. Planet Change* **113**, 91-109. https://doi.org/10.1016/j.gloplacha.2013.11.005.

Jochum, K.P., Stoll, B., Herwig, K., Willbold, M., Hofmann, A.W., Amini, M., Aarbug, S., Abouchami, W., Hellebrand, E., Mocek, B., Raczek, I., Stracke, A., Alard, O., Bouman, C., Becker, S., Dücking, M., Brätz, H., Klemd, R., de Bruin, D., Canil, D., Cornell, D., de Hoog, C.-S., Dalpé, C., Danyushevsky, L., Eisenhauer, A., Gao, Y., Snow, J.E., Groschopf, N., Günther, D., Latkoczy, C., Guillong, M., Hauri, E.K., Höfer, H.E., Lahaye, Y., Horz, K., Jacob, D.E., Kasemann, S.A., Kent, A.J.R., Ludwig, T., Zack, T., Mason, P.R.D., Meixner, A., Rosner, M., Kisawa, K., Nash, P.B., Pfänder, J., Premo, W.R., Sun, W.D., Tiepolo, M., Vannucci, R., Vennemann, T., Wayne, D., Woodhead, J.D., 2006. MPI-DING reference glasses for in situ microanalysis: New reference values for element concentrations and isotope ratios. *Geochem. Geophys.* **7**:2. https://doi.org/10.1029/2005GC001060.

Keller, J., Ryan, W.B.F., Ninkovich, D., Altherr, R., 1978. Explosive volcanic activity in the Mediterranean over the last 200,000 yr as recorded in deep-sea sediments. *Geol. Soc. Am. Bull.* **89**, 591-604. https://doi.org/10.1130/0016-7606(1978)89%3C591:EVAITM%3E2.0.CO;2.

Koppers, A.A.P., 2002. ArArCALC e software for $^{40}Ar/^{39}Ar$ age calculations. *Comput. Geosci.* **28**, 605-619. https://doi.org/10.1016/S0098-3004(01)00095-4.

Kuehn, S.C., Froese, D.G., Shane, P.A.R., INTAV Intercomparison Participants, 2011. The INTAV intercomparison of electron-beam microanalysis of glass by tephrochronology laboratories: Results and recommendations. *Quat. Int.* **246** (1-2), 19-47. https://doi.org/10.1016/j.quaint.2011.08.022.

Le Maitre, R.W., Streckeisen, A., Zanettin, B., Le Bas, M.J., Bonin, B., Bateman, P., Bellieni, G., Dudek, A., Efremova, S., Keller, J., Lameyre, J., Sabine, P.A., Schmid, R., SØrensen, H., Woolley, A.R., 2002. Igneous Rocks: A Classification and Glossary of Terms. Reccomendation of the International Union of Geological Sciences Subcommission on the Systematics of Igneous Rocks, 2nd Edition. Cambridge University Press, Cambridge. 236 pages.

Lee, J.Y., Marti, K., Severinghaus, J.P., Kawamura, K., Yoo, H.S., Lee, J.B., Kim, J.S., 2006. A redetermination of the isotopic abundances of atmospheric Ar. *Geochim. Cosmochim. Acta* **70** (17), 4507-4512. https://doi.org/10.1016/j.gca.2006.06.1563.

Leicher, Giaccio, B., Zanchetta, G., Sulpizio, R., Albert, P.G., Tomlinson, E.L., Lagos, M., Francke, A., Wagner, B., 2021. Lake Ohrid's tephrochronological dataset reveals 1.36 Ma of Mediterranean explosive volcanic activity. *Sci. Data* **8**, 231. https://doi.org/10.1038/s41597-021-01013-7.

Leicher, N., Zanchetta, G., Sulpizio, R., Giaccio, B., Wagner, B., Nomade, S., Francke, A., Del Carlo, P., 2016. First tephrostratigraphic results of the DEEP site record from Lake Ohrid (Macedonia and Alania). *Biogeosciences* **13**, 2151-2178. https://doi.org/10.5194/bg-13-2151-2016.

Lucchi, F., Keller, J., Tranne, C.A., 2013. Regional stratigraphic correlations across the Aeolian archipelago (southern Italy). In: Geological Society, London, Memoirs, vol. 37, Chapter 6, pp. 55-81. https://doi.org/10.1144/M37.6.

Ludwig, K.R., 2001. Isoplot 3.0a geochronological toolkit for Microsoft Excel. In: Special Publication No. 4. Berkeley Geochronology Center, Berkeley, CA, USA.

Marciano, R., Munno, R., Paola, P., Nicoletta, S., Santo, A., Villa, I., 2008. Late quaternary tephra layers along the Cilento coastline (southern Italy). *J. Volcanol. Geotherm. Res.* **177** (1), 227-243. https://doi.org/10.1016/j.jvolgeores.2007.11.009.

Marianelli, P. & Sbrana, A. Risultati di misure standard di minerali e di vetri naturali in microanalisi a dispersione di energia (In Italian). *Atti Soc. Tosc. Sci. Nat. Resid. Pisa, Mem. Serie A* **105**, 57-63 (1998).

Milner, A.M., Collier, R.E.L., Roucox, K.H., Müller, U.C, Pross, J., Kalaitzidis, S., Christanis, K., Tzedakis, P.C., 2012. Enhanced seasonality of precipitation in the Mediterranean during the early part of the Last Interglacial. *Geology* **40** (10), 919-922. https://doi.org/10.1130/G33204.1.

Milner, A.M., Müller, U.C., Roucoux, K.H., Collier, R.E., Pross, J., Kalaitzidis, S., Christanis, K., Tzedakis, P.C., 2013. Environmental variability during the Last Interglacial: a new high-resolution pollen record from Tenaghi Philippon, Greece. J. *Quat. Sci.* **28**, 113– 117. https://doi.org/10.1002/jqs.2617.

Milner, A.M., Roucoux, K.H., Collier, R.E. L., Müller, U.C., Pross, J., Tzedakis, P.C., 2016. Vegetation responses to abrupt climatic changes during the Last Interglacial Complex (Marine Isotope Stage 5) at Tenaghi Philippon, NE Greece. *Quat. Sci. Rev.* **154**, 169– 181. https://doi.org/10.1016/j.quascirev.2016.10.016.

Monaco, L., Palladino, D.M., Gaeta, M., Marra, F., Sottili, G., Leicher, N., Mannella, G., Nomade, S., Pereira, A., Regattieri, E., Wagner, B., Zanchetta, G., Albert, P.G., Arienzo, I., D'Antonio, M., Petrosino, P., Manning, C., Giaccio, B., 2021. Mediterranean tephrostratigraphy and peri-Tyrrhenian explosive activity revaluated in light of the 430-365 ka record from Fucino Basin (central Italy). *Earth Sci. Rev.* **220**, 103706. https://doi.org/10.1016/j.earscirev.2021.103706.

Morabito, S., Petrosino, P., Milia, A., Sprovieri, M., Tamburrino, S., 2014. A multidisciplinary approach for reconstructing the stratigraphic framework of the last 40 ka in a bathyal area of the eastern Tyrrhenian Sea. *Glob. Planet Change* **123** (A), 121-138. https://doi.org/10.1016/j.gloplacha.2014.10.005.

Munno, R. & Petrosino, P., 2007. The late Quaternary tephrostratigraphical record of the San Gregorio Magno basin (southern Italy). *J. Quat. Sci*. **22**, 247-266. https://doi.org/10.1002/jqs.1025.

North Greenland Ice-Core Project members, Andersen, K.K., Azuma, N., Barnola, J.M., Bigler, M., Biscaye, P., Caillon, N., Chappellaz, J., Clausen, H.B., Dahl-Jensen, D., Fischer, H., Flückiger, J., Fritzsche, D., Fujii, Y., Goto-Azuma, K., Grønvold, K., Gundestrup, N.S., Hansson, M., Huber, C., Hvidberg, C.S., Johnsen, S.J., Jonsell, U., Jouzel, J., Kipfstuhl, S., Landais, A.,Leuenberger, M., Lorrain, R., Masson-Delmotte, V., Miller, H., Motoyama, H., Narita, H., Popp, T., Rasmussen, S.O., Raynaud, D., Röthlisberger, R., Ruth, U., Samyn, D., Schwander, J., Shoji, H., Siggard-Andersen, M.L., Steffensen, J.P., Stocker, T., Sveinbjörnsdottir, A.E., Svensson, A., Takata, M., Tison, J. L., Thorsteinsson, T.,Watanabe, O., Wilhelms, F., White, J., 2004. High-resolution record of the Northern Hemisphere climate extending into the last interglacial period. *Nature* **431**, 147-151.

Niespolo, E.M., Rutte, D., Deino, A.L., Renne, P.R., 2017. Intercalibration and age of the Alder Creek Sanidine ^{40}Ar/^{39}Ar standard. *Quat. Geochronol.* **39**, 205-213. https://doi.org/10.1016/j.quageo.2016.09.004.

Pabst, S., Wörner, G., Civetta, L., Tesoro, R., 2007. Magma chamber evolution prior to the Campanian Ignimbrite and Neapolitan Yellow Tuff eruptions (Campi Flegrei, Italy). *Bull. Volcanol.* **70**, 961-976. https://doi.org/10.1007/s00445-007-0180-z.

Pappalardo, L., Civetta, L., D'Antonio, M., Deino, A., Di Vito, M., Orsi, G., Carandente, A., de Vita, S., Isaia, R., Piochi, M., 1999. Chemical and Sr-isotopical evolution of the Phlegrean magmatic system before the Campanain Ignimbrite and the Neapolitan Yellow Tuff eruptions. *J. Volcanol. Geotherm. Res.* **91** (2-4), 141-166. https://doi.org/10.1016/S0377-0273(99)00033-5.

Paterne, M., Guichard, F., Duplessy, J.C., Siani, G., Sulpizio, R., Labeyrie, J., 2008. A 90,000-200,000 yrs marine tephra record of Italian volcanic activity in the Central Mediterranean Sea. J. *Volcanol. Geotherm. Res.* **177**, 187-196. https://doi.org/10.1016/j.jvolgeores.2007.11.028.

Paterne, M., Guichard, F., Labeyrie, J., 1988. Explosive activity of the south Italian volcanoes during the past 80,000 years as determined by marine tephrochronology. *J. Volcanol. Geotherm. Res.* **34**, 153-172. https://doi.org/10.1016/0377-0273(88)90030-3.

Paterne, M., Guichard, F., Labeyrie, J., Gillot, P.Y., Duplessy, J.C., 1986. Tyrrhenian Sea tephrochronology of the oxygen isotope record for the past 60,000 years. *Mar. Geol.* **72**, 259-285. https://doi.org/10.1016/0025-3227(86)90123-4.

Pelullo, C., Cirillo, G., Iovine, R.S., Arienzo, I., Aulinas, M., Pappalardo, L., Petrosino P., Fernandez-Turiel, J.L., D'Antonio, M., 2020. Geochemical and Sr-Nd isotopic features of the Zaro volcanic complex: insights on the magmatic processes triggering a small-scale prehistoric eruption at Ischia island (south Italy). *Int. J. Earth Sci.* **109** (8), 2829-2849. https://doi.org/10.1007/s00531-020-01933-6.

Peccerillo, A., 2017. Cenozoic Volcanism in the Tyrrhenian Sea Region. In: IAVCEI, Advances in Volcanology, 2 ed. Springer, p. 400.

Petrosino, P., Arienzo, I., Mazzeo, F.C., Natale, J., Petrelli, M., Milia, A., Perugini, D., D'Antonio, M., 2019. The San Gregorio Magno lacusrine basin (Campania, southern Italy): improved characterization of the tephrostratigraphic markers based on trace elements and isotopic data. *J. Quat. Sci.* **34**, 393-404. https://doi.org/10.1002/jqs.3107.

Petrosino, P., Jicha, B.R., Mazzeo, F.C., Ciaranfi, N., Girone, A., Maiorano, P., 2015. The Montalbano Jonico marine succession: An archive for distal tephra layers at the Early-Middle Pleistocene boundary in southern Italy. *Quat. Int*. **383**, 89-103. https://doi.org/10.1016/j.quaint.2014.10.049.

Petrosino, P., Morabito, S., Jicha, B.R., Milia, A., Sprovieri, M., Tamburrino, S., 2016. Multidisciplnary tephrochronological correlation of marker events in the eastern Tyrrhenian Sea between 48 and 105 ka. *J. Volcanol. Geotherm. Res.* **315**, 79-99. https://doi.org/10.1016/j.jvolgeores.2016.02.001.

Poli, S., Chiesa, S., Gillot, P.-Y., Gregnanin, A., Guichard, F., 1987. Chemistry versus time in the volcanic complex of Ischia (Gulf of Naples, Italy): evidence of successive magmatic cycles. *Contrib. Mineral. Petrol.* **95**, 322-335.

Rasmussen, S.O., Bigler, M., Blockley, S.P., Blunier, T., Buchardt, S.L., Clause, H.B., Cvijanovic, I., Dahl-Jensen, D., Johnsen, S.J., Fischer, H., Gkinis, V., Guillevic, M., Hoek, W.Z., Lowe, J.J., Pedro, J.B., Popp, T., Seierstad, I.K., Steffensen, J.P., Svensson, A.M., Vallelonga, P., Vinther, P.M., Walker, M.J.C., Wheatley, J.J., Winstrup, M., 2014. A stratigraphic framework for abrupt climatic changes during the Last Glacial period based on three synchronized Greenland ice-core records: refining and extending the INITIMATE event stratigraphy. *Quat. Sci. Rev.* **106**, 14-28. https://doi.org/10.1016/j.quascirev.2014.09.007.

Regattieri, E., Giaccio, B., Nomade, S., Francke, A., Vogel, H., Drysdale, R.N., Perchiazzi, N., Wagner, B., Gemelli, M., Mazzini, I., Boschi, C., Galli, P., Peronace, E., 2017. A Last Interglacial record of environmental changes from the Sulmona Basin (central Italy). *Palaeogeogr. Palaeoclimatol. Palaeoecol.* **472**, 51-66. https://doi.org/10.1016/j.palaeo.2017.02.013.

Regattieri, E., Giaccio, B., Zanchetta, G., Drysdale, R.N., Galli, P., Nomade, S., Peronace, E., Wulf, S., 2015. Hydrological variability over the Apennines during the Early Last Glacial precession minimum, as revelated by a stable isotope record from Sulmona basin, Central Italy. *J. Quat. Sci.* **30**, 19-31. https://doi.org/10.1002/jqs.2755.

Renne, P.R., Balco, G., Ludwig, K.R., Mundil, R., Min, K., 2011. Response to the comment by WH Schwarz et al. on "Joint determination of 40 K decay constants and $^{40}Ar^*/^{40}K$ for the Fish Canyon sanidine standard, and improved accuracy for $^{40}Ar/^{39}Ar$ geochronology" by PR Renne et al. (2010). *Geochim. Cosmochim. Acta* **75**, 5097-5100.

Rolandi, G., Bellucci, F., Heizler, M.T., Belkin, H.E., De Vivo, B., 2003. Tectonic controls on the genesis of ignimbrite from the Campanian Volcanic Zone, southern Italy. *Mineral. Petrol.* **79**, 3-31. https://doi.org/10.1007/s00710-003-0014-4.

Rosi, M., Sbrana, A., Vezzoli, L., 1988a. Tephrostratigraphy of Ischia, Procida and Campi Flegrei volcanic products (In Italian). *Mem. Soc. Geol. It.* **41**, 1015-1027.

Rosi, M., Sbrana, A., Vezzoli, L., 1988b. Stratigraphy of Procida and Vivara islands (In Italian). *Boll. GNV* **4**, 500-525.

Santacroce, R. & Sbrana, A., 2003. Geological map of Vesuvius, 1:15.000 scale. SELCA, Firenze.

Santacroce, R., Cioni, R., Marianelli, P., Sbrana, A., Sulpizio, R., Zanchetta, G., Donahue, D.J., Joron, J.L., 2008. Age and whole rock-glass compositions of proximal pyroclastics from the major explosive eruptions of Somma-Vesuvius: A review as a tool for distal tephrostratigraphy. *J. Volcanol. Geotherm. Res.* **177**, 1-18. https://doi.org/10.1016/j.jvolgeores.2008.06.009.

Satow, C., Tomlinson, E.L., Grant, K.M., Albert, P.G., Smith, V.C., Manning, C.J., Ottolini, L., Wulf, S., Rohling, E.J., Lowe, J.J., Blockley, S.P.E., Menzies, M.A., 2015. A new contribution to the Late Quaternary tephrostratigraphy of the Mediterranean: Aegean Sea core LC21. *Quat. Sci. Rev.* **117**, 96-112. https://doi.org/10.1016/j.quascirev.2015.04.005.

Scarpati, C., Perrotta, A., Lepore, S., Calvert, A. 2013. Eruptive history of the Neapolitan volcanoes: constraints from ^{40}Ar-^{39}Ar dating. *Geol. Mag.* **150** (3), 412-425. https://doi.org/10.1017/S0016756812000854.

Shackleton, N.J., Fairbanks, R.G., Chiu, T., Parennin, F., 2004. Absolute calibration of the Greenland time scale: implications for the Antarctic time scales and for $\Delta^{14}C$. *Quat. Sci. Rev*. **23** (14-15), 1513-1522. https://doi.org/10.1016/j.quascirev.2004.03.006.

Sinopoli, G., Masi, A., Regattieri, E., Wagner, B., Francke, A., Peyron, O., Sadori, L., 2018. Palynology of the Last Interglacial Complex at Lake Ohrid: palaeoenvironmental and palaeoclimatic inferences. *Quat. Sci. Rev.* **180**, 177-192. https://doi.org/10.1016/j.quascirev.2017.11.013.

Smith, V.C., Isaia, R., Engwell, S.L., Albert, P.G., 2016. Tephra dispersal during the Campanian Ignimbrite (Italy) eruption: implications for ultra-distal ash transport during the large caldera-forming eruption. *Bull. Volcanol.* **78**, 45. https://doi.org/10.1007/s00445-016-1037-0.

Smith, V.C., Isaia, R., Pearce, N.J.G., 2011. Tephrostratigrapy and glass compositions of post-15 kyr Campi Flegrei eruptions: implications for eruption history and chronostratigraphic markers. *Quat. Sci. Rev.* **30**, 3638-3660.

Sulpizio, R., Zanchetta, G., D'Orazio, M., Vogel, H., Wagner, B., 2010. Tephrostratigraphy and tephrochronology of lakes Ohrid and Prespa, Balkans. *Biogeosciences* **7**, 3273-3288. https://doi.org/10.5194/bg-7-3273-2010.

Tomlinson, E.L., Albert, P.G., Wulf, S., Brown, R.J., Smith, V.C., Keller, J., Orsi, G., Bourne, A., Menzies, M.A., 2014. Age and geochemistry of tephra layers from Ischia, Italy: constraints from proximal-distal correlations with Lago Grande di Monticchio. *J. Volcanol. Geotherm. Res.* **287**, 22-39. https://doi.org/10.1016/j.jvolgeores.2014.09.006.

Tomlinson, E.L., Arienzo, I., Civetta, L., Wulf, S., Smith, V.C., Hardiman, M., Lane, C.S., Carandente, A., Orsi, G., Rosi, M., Müller, W., Menzies, M.A., 2012. Geochemistry of the Phlegrean Fields (Italy) proximal sources for major Mediterranean tephras: Implications for the dispersal of Plinian and co-ignimbritic components of explosive eruptions. *Geochim. Cosmochim. Acta* **93**, 102-128. https://doi.org/10.1016/j.gca.2012.05.043.

Tomlinson, E.L., Thordarson, T., Muller, W., Thirlwall, M.T., Menzies, M.A., 2010. Microanalysis of tephra by LA-ICP-MS - strategies, advantages and limitations assessed using the Thorsmork ignimbrite (Southern Iceland). *Chem. Geol.* **279**, 73-89. https://doi.org/10.1016/j.chemgeo.2010.09.013.

Tonarini, S., D'Antonio, M., Di Vito, M.A., Orsi, G., Carandente, A., 2009. Geochemical and Ba-Sr-Nd isotopic evidence for mingling and mixing processes in the magmatic system that fed the Astroni volcano (4.1-3.8 ka) within the Campi Flegrei caldera (southern Italy). *Lithos* **107** (3-4), 135-151. https://doi.org/10.1016/j.lithos.2008.09.012.

Wagner, B., Wilke, T., Francke, A., Albrecht, C., Baumgarten, H., Bertini, A., Combourieu-Nebout, N., Cvetkoska, A., D'Addabbo, M., Donders, T.H., Föller, K., Giaccio, B., Grazhdani, A., Hauffe, T., Holtvoeth, J., Joannin, S., Jovanovska, E., Lust, J., Kouli, K., Koutsodendris, A., Krastel, S., Lacey, J.H., Leicher, N., Leng, M.J., Levkov, Z., Lindhorst, K., Masi, A., Mercuri, A.M., Nomade, S., Nowaczyk, N., Panagiotopoulos, K., Peyron, O., Reed, J.M., Regattieri, E., Sadori, L., Sagnotti, L., Stelbrink, B., Sulpizio, R., Tofilovska, S., Torri, P., Vogel, H., Wagner, T., Wagner-Cremer, F., Wolff, G.A., Wonik, T., Zanchetta, G., Zhang, X.S., 2017. The environmental and evolutionary history of Lake Ohrid (FYROM/Albania): interim results from the SCOPSCO deep drilling project. *Biogeosciences* **14**, 2033-2054. https://doi.org/10.5194/bg-14-2033-2017.

Wagner, B., Vogel, H., Francke, A., Friederich, T., Donders, T., Lacey, J.H., Leng, M.J., Regattieri, E., Sadori, L., Wilke, T., Zanchetta, G., Albrecht, C., Bertini, A., Combourieu-Nebout, N., Cvetkoska, A., Giaccio, B., Grazhdani, A., Hauffe, T., Holtvoeth, J., Joannin, S., Lagoos, M., Leicher, N., Levkov, Z., Lindhorst, K., Masi, A., Melles, M., Mercuri, A.M., Nomade, S., Nowaczyk, N., Panagiotopoulos, K., Peyron, O., reed, J.M., Sagnotti, L., Sinopoli, G., Stellbrink, B., Sulpizio, R., Timmermann, A., Tofilovska, S., Torri, P., Wagner-Cremer, F., Wonik, T., Zhang, X., 2019. Mediterranean winter rainfall in phase with African monsoons during the past 1.36 million years. *Nature* **573**, 256-260. https://doi.org/10.1038/s41586-019-1529-0.

Wulf, S., Hardiman, M.J., Staff, R.A., Koutsodendris, A., Appelt, O., Blockley, S.P.E., Lowe, J.J., Manning, C.J., Ottolini, L., Schmitt, A.K., Smith, V.C., Tomlinson, E.L., Vakhrameeva, P., Knipping, M., Kotthoff, U., Milner, A.M., Müller, U.C., Christanis, K., Kalaitzidis, S., Tzedakis, P.C., Schmiedl, G., Pross, J., 2018. The Marine isotope stage 1-5 cryptotephra record of Tenaghi Philippon, Greece: Towards a detailed tephrostratigraphic framework for the Eastern Mediterranean region. *Quat. Sci. Rev.* **186**, 236-262. https://doi.org/10.1016/j.quascirev.2018.03.011.

Wulf, S., Keller, J., Paterne, M., Mingram, J., Lauterbach, S., Opitz, S., Sottili, G., Giaccio, B., Albert, P.G., Satow, C., Tomlinson, E.L., Viccaro, M., Brauer, A., 2012. The 100-133 ka record of Italian explosive volcanism and revised tephrochronology of Lago Grande di Monticchio. *Quat. Sci. Rev.* **58**, 104-123. https://doi.org/10.1016/j.quascirev.2012.10.020.

Wulf, S., Kraml, M., Keller, J., 2008. Towards a detailed tephrostratigraphy in the Central Mediterranean: The last 20,000 yrs record of Lago Grande di Monticchio. J. *Volcanol. Geotherm. Res.* **177**, 118-132. https://doi.org/10.1016/j.jvolgeores.2007.10.009.

Wulf, S., Kraml., M., Brauer, A., Keller, J., Negendank, J.F.W., 2004. Tephrochronology of the 100 ka lacustrine sediment record of Lago Grande di Monticchio (Southern Italy). *Quat. Int*. **122**, 7-30. https://doi.org/10.1016/j.quaint.2004.01.028.

Zanchetta, G., Giaccio, B., Bini, M., Sarti, L., 2018. Tephrostratigraphy of Grotta del Cavallo, Southern Italy: insights of the chronology of Middle to Upper Paleolithic transition in the Mediterranean. *Quat. Sci. Rev.* **182**, 65-77. https://doi.org/10.1016/j.quascirev.2017.12.014.

Ziegler, M., Tuenter, E., Lourens, L.J. 2010. The precession phase of the boreal summer monsoon as viewed from the eastern Mediterranean (ODP Site 968). *Quat. Sci. Rev*. **29** (11-12), 1481-1490. https://doi.org/10.1016/j.quascirev.2010.03.011.

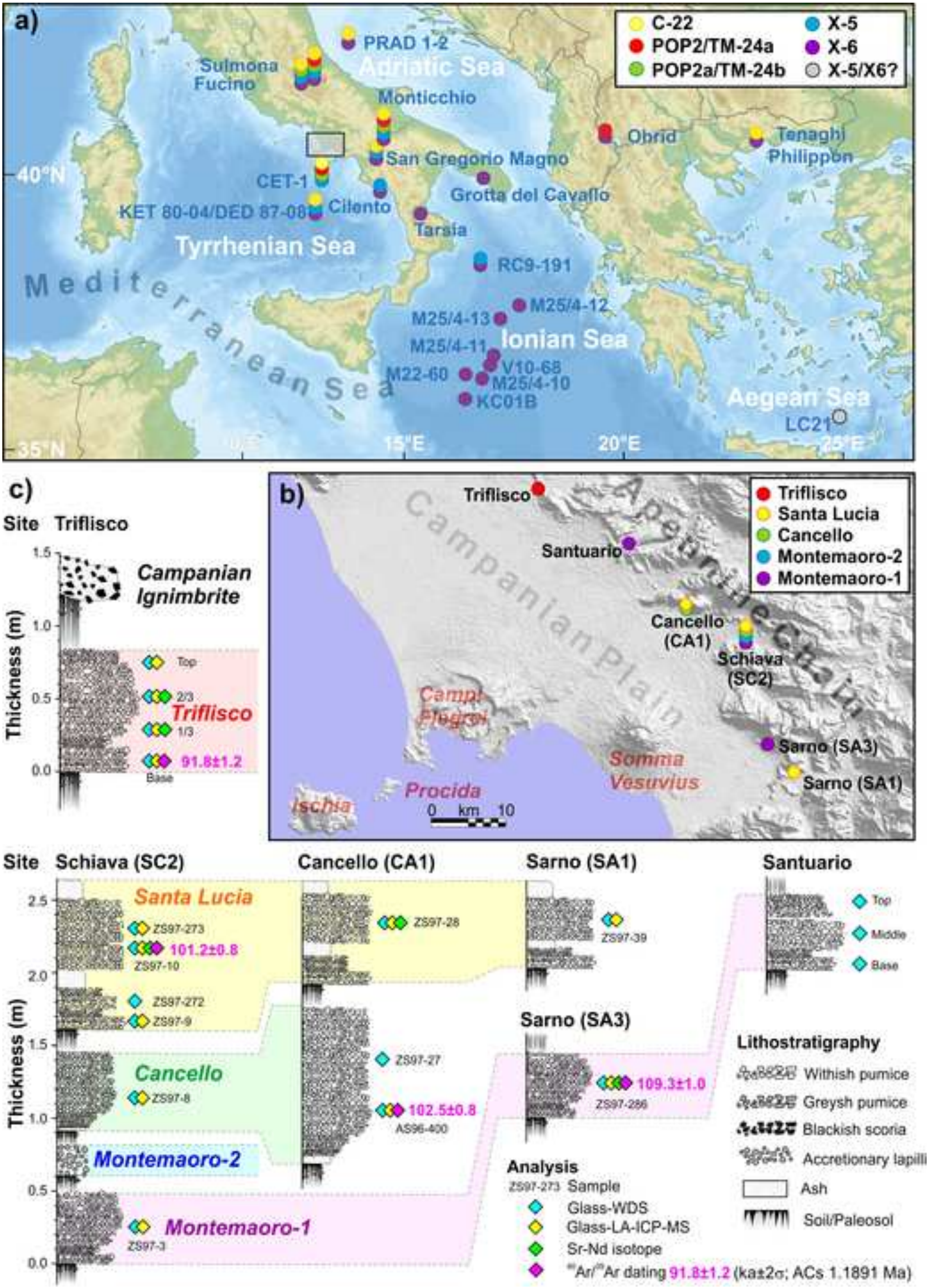

a)
C-22
POP2/TM-24a
POP2a/TM-24b
X-5
X-6
X-5/X6?
PRAD 1-2
Adriatic Sea
Sulmona
Fucino
Monticchio
Obrid
Tenaghi Philippon
San Gregorio Magno
40°N
CET-1
Grotta del Cavallo
KET 80-04/DED 87-08
Cilento
Tarsia
Tyrrhenian Sea
RC9-191
Mediterranean Sea
M25/4-12
M25/4-13
Ionian Sea
M25/4-11
V10-68
M22-60
M25/4-10
KC01B
Aegean Sea
LC21
35°N
15°E
20°E
25°E
b)
Triflisco
Santuario
Campanian Plain
Apennine Chain
Triflisco
Santa Lucia
Cancello
Montemaoro-2
Montemaoro-1
Cancello (CA1)
Schiava (SC2)
Campi Flegrei
Sarno (SA3)
Sarno (SA1)
Somma Vesuvius
Procida
Ischia
0 km 10
c)
Site Triflisco
Campanian Ignimbrite
Thickness (m)
Top
2/3
1/3
Base
Triflisco
91.8±1.2
Site Schiava (SC2)
Cancello (CA1)
Sarno (SA1)
Santuario
Santa Lucia
ZS97-273
101.2±0.8
ZS97-10
ZS97-272
ZS97-9
ZS97-28
ZS97-39
Top
Middle
Base
Cancello
ZS97-8
ZS97-27
102.5±0.8
AS96-400
Sarno (SA3)
109.3±1.0
ZS97-286
Montemaoro-2
Montemaoro-1
ZS97-3
Lithostratigraphy
Withish pumice
Greysh pumice
Blackish scoria
Accretionary lapilli
Ash
Soil/Paleosol
Analysis
ZS97-273 Sample
Glass-WDS
Glass-LA-ICP-MS
Sr-Nd isotope
40Ar/39Ar dating 91.8±1.2 (ka±2σ; ACs 1.1891 Ma)

Figure

Click here to access/download;Figure;Figure. 2.jpg

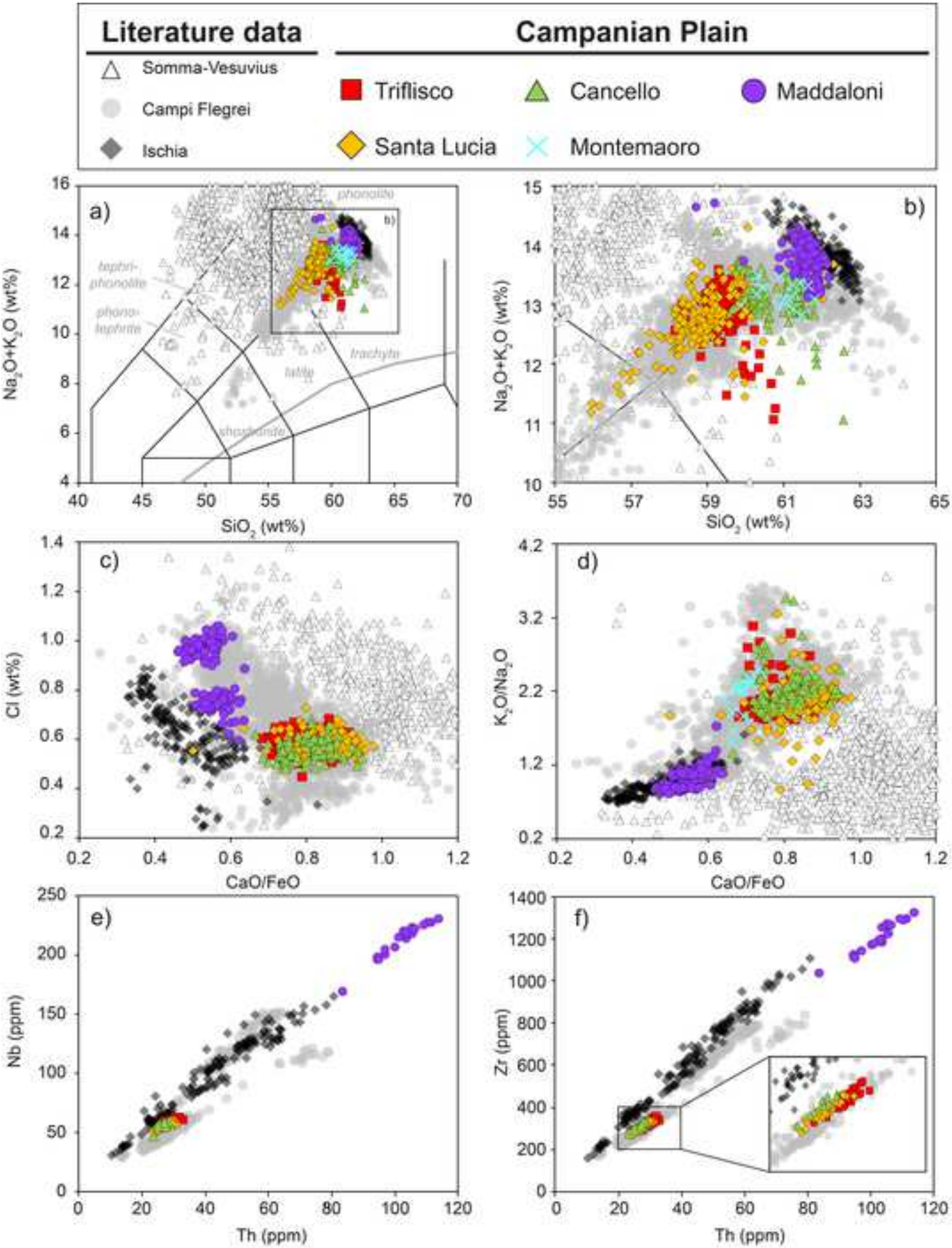

Figure Click here to access/download;Figure;Figure. 3.jpg

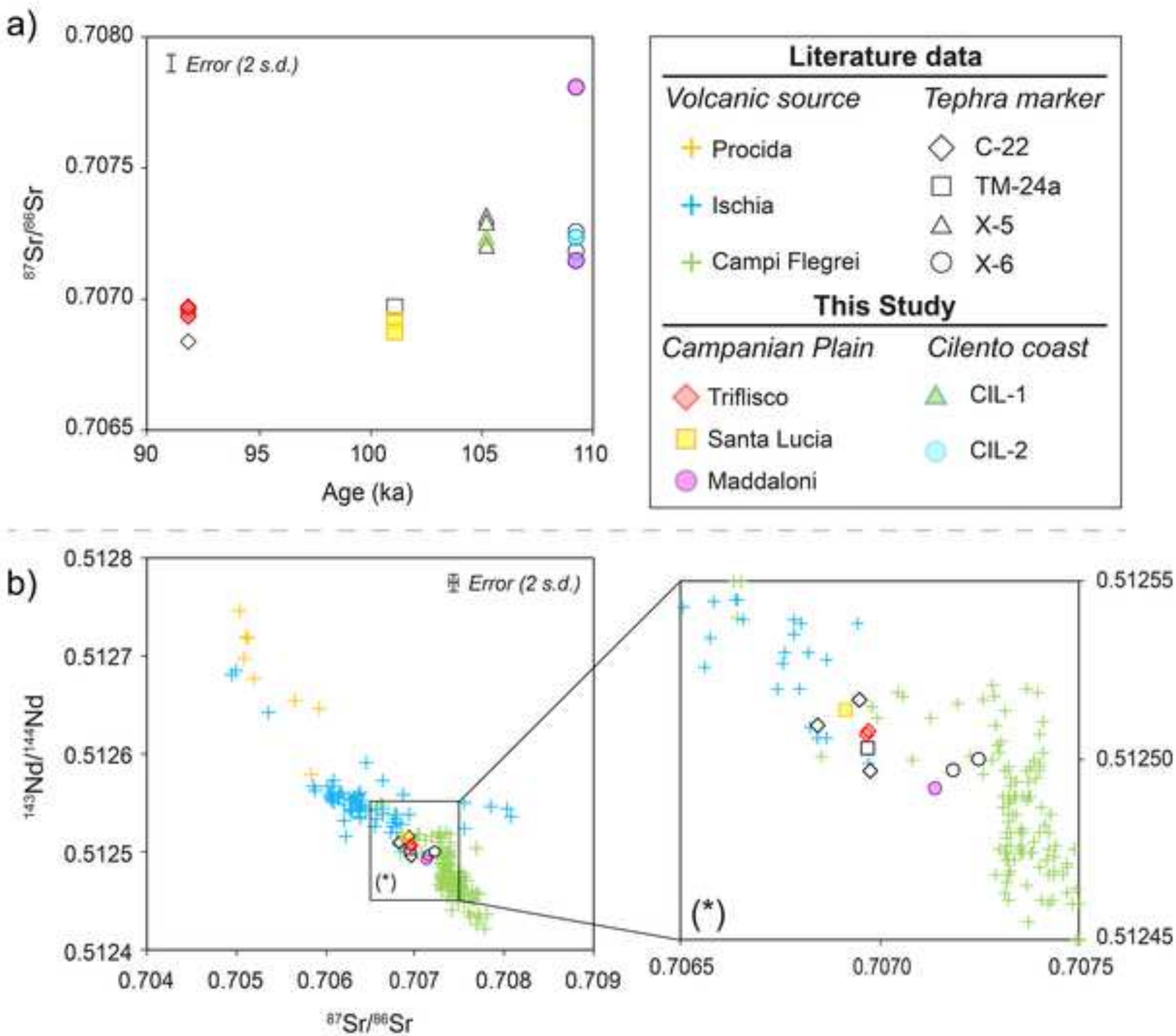

Figure

Click here to access/download;Figure;Figure. 4.jpg

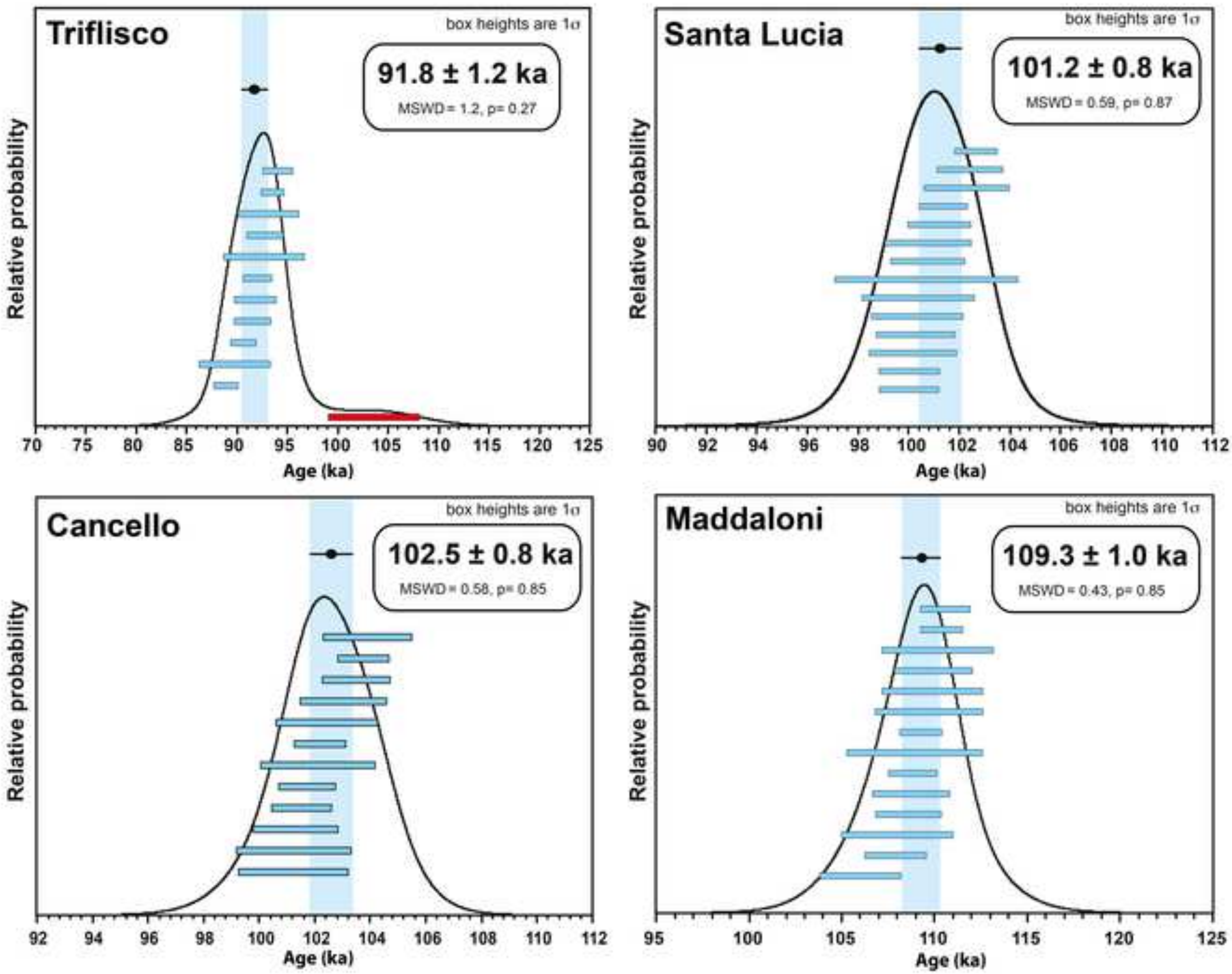

Figure Click here to access/download;Figure;Figure. 5.jpg

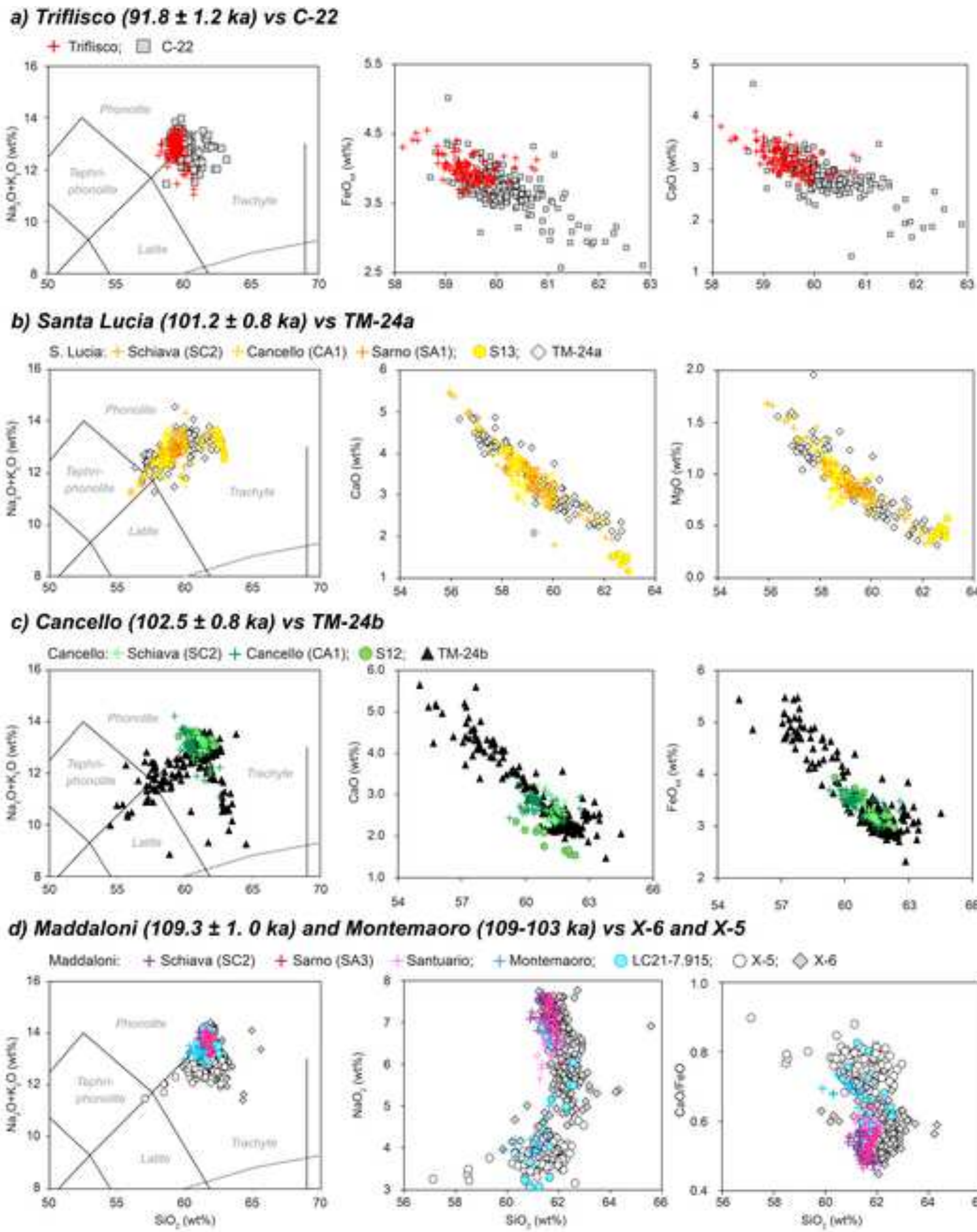

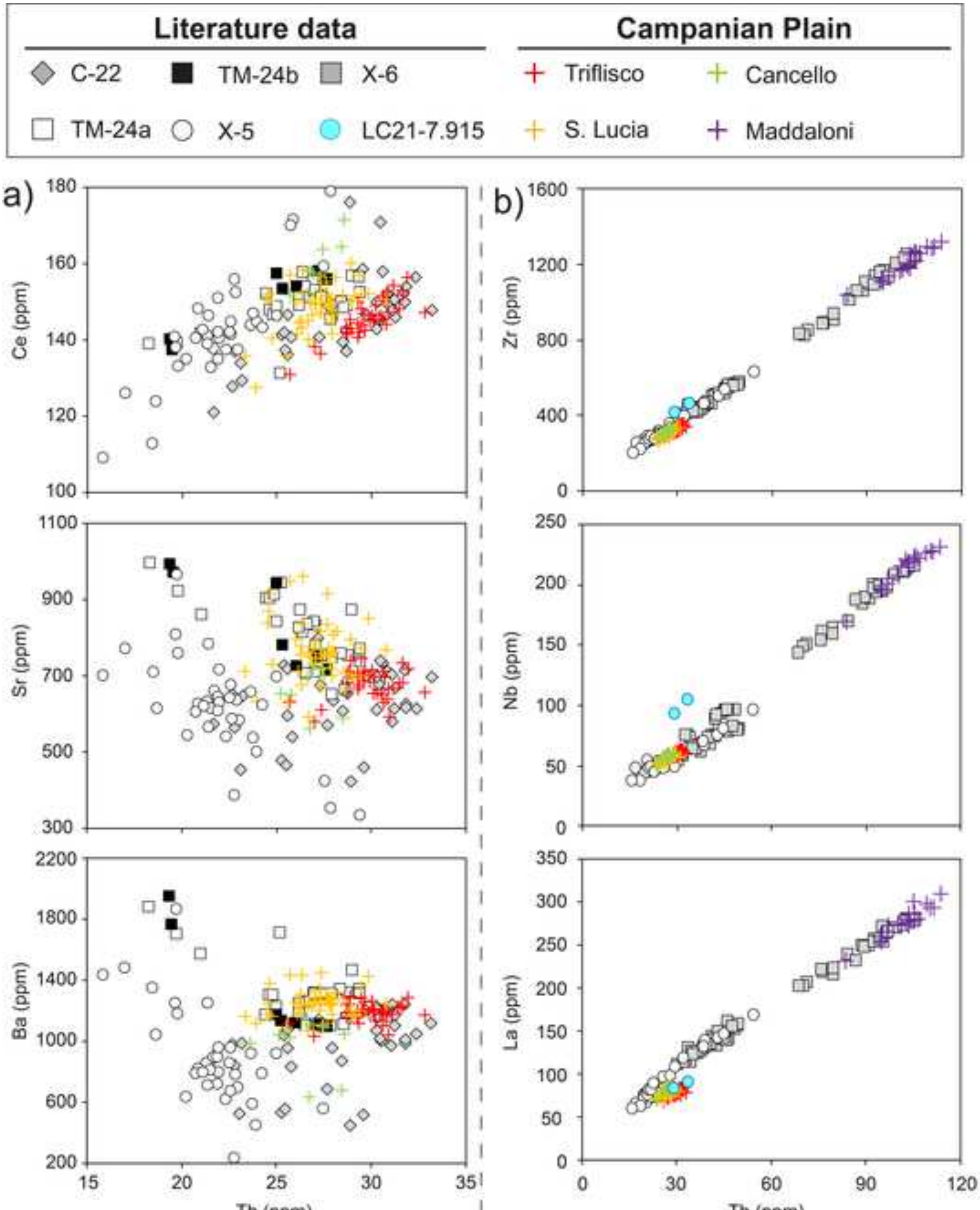
Literature data
C-22
TM-24b
X-6
TM-24a
X-5
LC21-7.915
Campanian Plain
Triflisco
Cancello
S. Lucia
Maddaloni
a)
b)
Ce (ppm)
Sr (ppm)
Ba (ppm)
Th (ppm)
Zr (ppm)
Nb (ppm)
La (ppm)
Th (ppm)

Figure Click here to access/download;Figure;Figure. 7.jpg

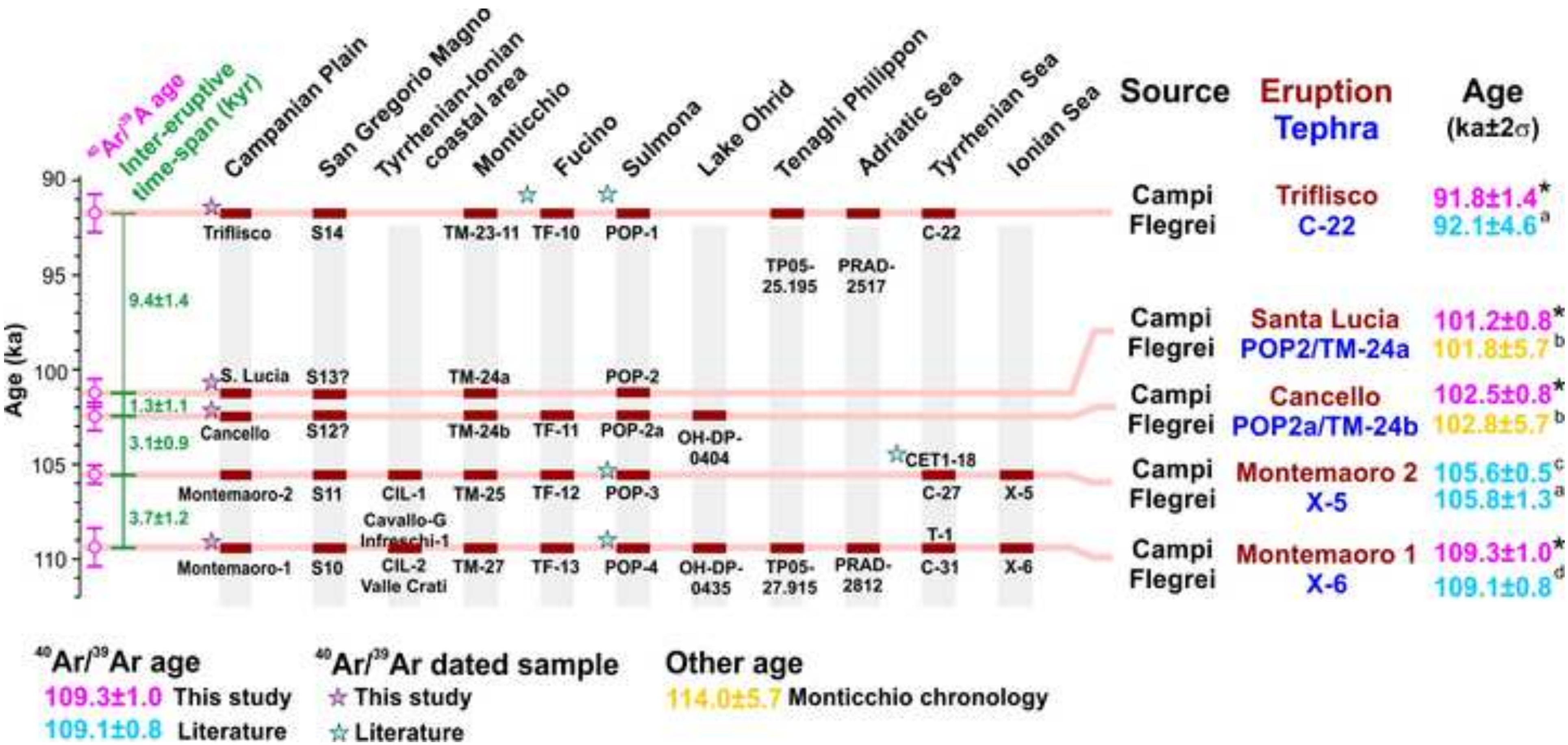

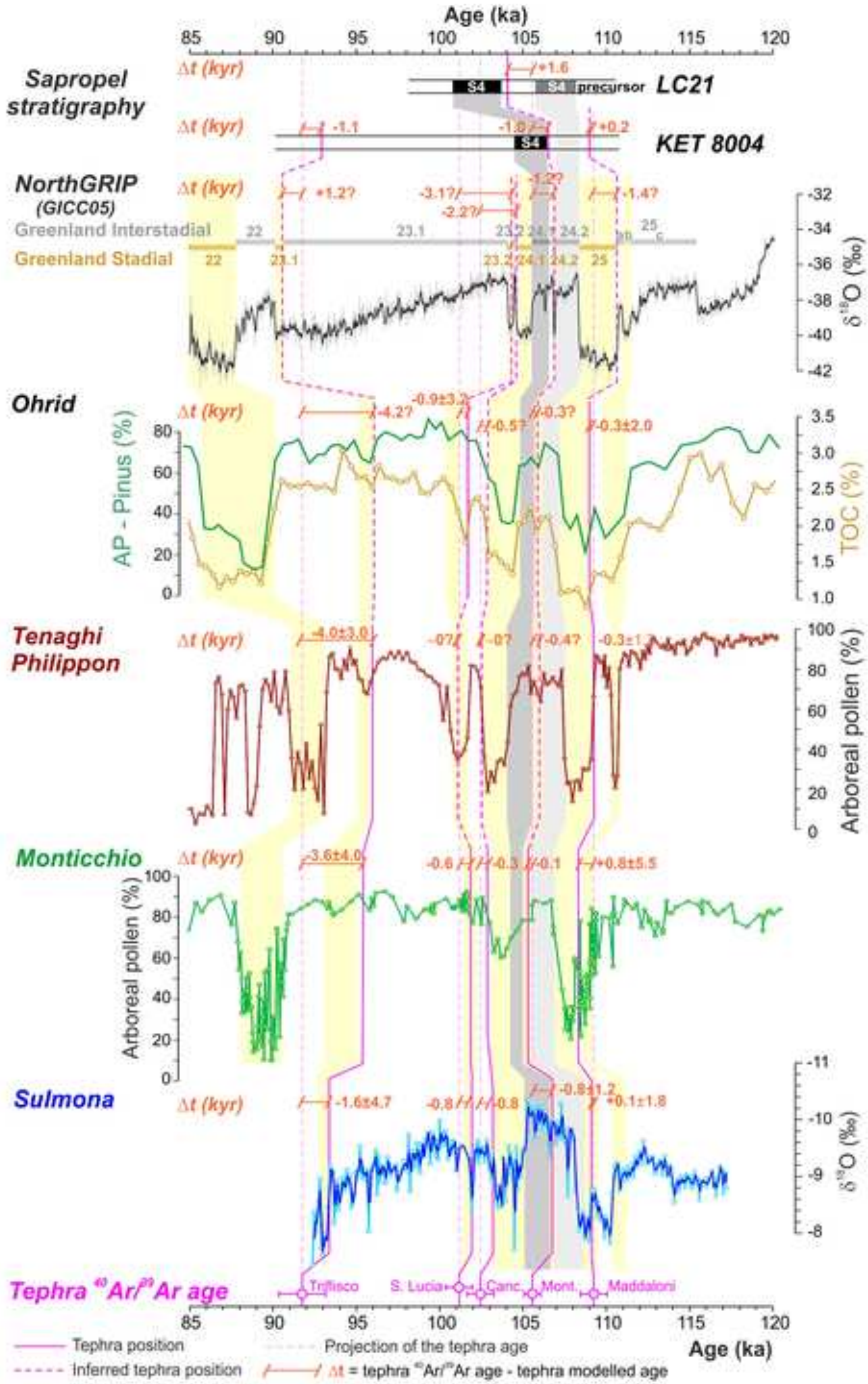
Age (ka)
85 90 95 100 105 110 115 120
Sapropel stratigraphy
Δt (kyr)
LC21
S4
S4 precursor
KET 8004
NorthGRIP (GICC05)
Greenland Interstadial
Greenland Stadial
δ18O (‰)
Ohrid
AP - Pinus (%)
TOC (%)
Tenaghi Philippon
Arboreal pollen (%)
Monticchio
Arboreal pollen (%)
Sulmona
δ18O (‰)
Tephra 40Ar/39Ar age
Triflisco
S. Lucia
Canc.
Mont.
Maddaloni
Tephra position
Inferred tephra position
Projection of the tephra age
Δt = tephra 40Ar/39Ar age - tephra modelled age